

## RESEARCH ARTICLE

# Novel track morphotypes from new tracksites indicate increased Middle Jurassic dinosaur diversity on the Isle of Skye, Scotland

Paige E. dePolo<sup>1\*</sup>, Stephen L. Brusatte<sup>1</sup>, Thomas J. Challands<sup>1</sup>, Davide Foffa<sup>2</sup>, Mark Wilkinson<sup>1</sup>, Neil D. L. Clark<sup>3</sup>, Jon Hoad<sup>4</sup>, Paulo Victor Luiz Gomes da Costa Pereira<sup>5</sup>, Dugald A. Ross<sup>6</sup>, Thomas J. Wade<sup>1</sup>

**1** School of GeoSciences, University of Edinburgh, Edinburgh, Scotland, United Kingdom, **2** National Museums Scotland, Edinburgh, Scotland, United Kingdom, **3** The Hunterian, University of Glasgow, Glasgow, Scotland, United Kingdom, **4** Art of Ancient Life Limited, Perth, Scotland, United Kingdom, **5** Departamento de Geologia, Universidade Federal do Rio de Janeiro, Rio de Janeiro, Brazil, **6** Staffin Museum, Staffin, Isle of Skye, Scotland, United Kingdom

☉ These authors contributed equally to this work.

‡ These authors also contributed equally to this work.

\* [paige.depolo@ed.ac.uk](mailto:paige.depolo@ed.ac.uk)



## OPEN ACCESS

**Citation:** dePolo PE, Brusatte SL, Challands TJ, Foffa D, Wilkinson M, Clark ND, et al. (2020) Novel track morphotypes from new tracksites indicate increased Middle Jurassic dinosaur diversity on the Isle of Skye, Scotland. PLoS ONE 15(3): e0229640. <https://doi.org/10.1371/journal.pone.0229640>

**Editor:** Anthony R. Fiorillo, Perot Museum of Nature and Science, UNITED STATES

**Received:** March 30, 2019

**Accepted:** February 11, 2020

**Published:** March 11, 2020

**Copyright:** © 2020 dePolo et al. This is an open access article distributed under the terms of the [Creative Commons Attribution License](https://creativecommons.org/licenses/by/4.0/), which permits unrestricted use, distribution, and reproduction in any medium, provided the original author and source are credited.

**Data Availability Statement:** All photogrammetric models and photosets used to construct them are available from the Dryad database (10.5061/dryad.n6f068k)

**Funding:** PEDP's Master's work was supported by a student award from the Association of Women Geoscientists (AWG). Fieldwork funding was provided by the National Geographic Society [GEFNE185-16] (awarded to SLB), Derek and Maureen Moss, the Edinburgh Zoo and the

## Abstract

Dinosaur fossils from the Middle Jurassic are rare globally, but the Isle of Skye (Scotland, UK) preserves a varied dinosaur record of abundant trace fossils and rare body fossils from this time. Here we describe two new tracksites from Rubha nam Braithairean (Brothers' Point) near where the first dinosaur footprint in Scotland was found in the 1980s. These sites were formed in subaerially exposed mudstones of the Lealt Shale Formation of the Great Estuarine Group and record a dynamic, subtropical, coastal margin. These tracksites preserve a wide variety of dinosaur track types, including a novel morphotype for Skye: *Del-tapodus* which has a probable stegosaur trackmaker. Additionally, a wide variety of tridactyl tracks shows evidence of multiple theropods of different sizes and possibly hints at the presence of large-bodied ornithopods. Overall, the new tracksites show the dinosaur fauna of Skye is more diverse than previously recognized and give insight into the early evolution of major dinosaur groups whose Middle Jurassic body fossil records are currently sparse.

## Introduction

Dinosaur fossils are sparse from the Middle Jurassic (174–164 Ma) [1]. However, the fossiliferous Great Estuarine Group which crops out in the Hebrides of Scotland, UK, spans this time period [2]. Both body and trace fossils found in the Hebrides, particularly on the Isle of Skye, have the potential to fill in gaps in our understanding of dinosaurs during this critical time in their evolution when sauropods, theropods, and thyreophorans all experienced evolutionary radiations [3–7].

The Great Estuarine Group of Skye has yielded isolated dinosaur body fossils including sauropod teeth and limb bones, theropod teeth and vertebrae, and a thyreophoran ulna and radius [8–14]. Skye preserves evidence of vibrant terrestrial and marine ecosystems that, in addition

Edinburgh Geological Society. The funders had no role in study design, data collection and analysis, decision to publish, or preparation of the manuscript. JH is self-employed at the freelance art studio, Art of Ancient Life Limited, but did not receive financial compensation for participation in this research. The specific roles of all authors are articulated in the 'author contributions' section.

**Competing interests:** JH is self-employed at the freelance art studio, Art of Ancient Life Limited, this affiliation does not alter our adherence to PLOS ONE policies on sharing data and materials

**Abbreviations:** GLAHM, The Hunterian, University of Glasgow, Glasgow, Scotland, UK; UCMP, University of California Museum of Paleontology, Berkeley, California, USA.

to dinosaurs, included sharks, ichthyosaurs, plesiosaurs, salamanders, turtles, crocodylomorphs, tritylodonts, and docodonts [15–20].

By far, however, the most common dinosaur fossils on Skye are tracks. They are often found on intertidal platforms, primarily along the northern coast of the island [21 and references therein]. The first Scottish dinosaur fossil reported was a single isolated footprint (GLAHM V1980), which had fallen from the cliffs at Rubha nam Brathairean (Brothers' Point), on the Trotternish Peninsula of Skye [22]. Since that time, several other tracksites have been discovered across the island, including well-known trackways at Staffin [23] and Duntulm [24] that are visible *in-situ* and have become popular tourist attractions. Most recently, our team has described a new site with sauropod and theropod tracks from Rubha nam Brathairean (the 'Brothers' Point 2' site), geographically close to where the first isolated track was found, but likely from a different stratigraphic horizon [25].

Here we describe two new dinosaur tracksites from Rubha nam Brathairean (hereafter called by its English name, Brothers' Point). These tracksites preserve a novel track morphology of a probable stegosaur that was hitherto unknown from Skye and which also represents one of the oldest fossil records of this major dinosaur group from anywhere in the world. These new tracksites complement the sparse dinosaur body fossil record of Skye and further illustrate the high diversity of dinosaurs on the island during the Middle Jurassic.

## Discovery of the tracksites

The two tracksites we describe here are referred to as Brothers' Point 1 (BP1) and Brothers' Point 3 (BP3). As mentioned above, another tracksite from the same area, denoted as Brothers' Point 2, which preserves sauropod and theropod tracks made in a shallow lagoon, was described separately in [25]. All three tracksites were discovered during fieldwork on the Isle of Skye by the PalAlba consortium of Scottish-based paleontologists. The numbering scheme refers to the order in which the three sites were found, over the course of fieldwork from 2015–2017.

BP1 was discovered in the autumn of 2015 by Thomas Challands while prospecting with Neil Clark. BP3 was discovered in May 2017, by Paulo Pereira, while prospecting as part of a large PalAlba fieldtrip funded by the National Geographic Society. Both sites were subsequently mapped and studied in detail by Paige dePolo as part of her MScR. thesis at the University of Edinburgh [26].

## Geological context

The Inner Hebrides, an island archipelago off the west coast of Scotland, feature one of the most complete sequences of Middle Jurassic sedimentary rocks in the world [27]. A series of formations, known collectively as the Great Estuarine Group, record repeated cycles of delta progradation and retrogradation into marine-influenced lagoons, during the Bajocian-Bathonian (ca. 170–166 million years ago) [28]. The dating of these rocks has proved challenging historically because they do not preserve the correct depositional environments for ammonites, which are the most relevant index fossils [29]. However, their stratigraphic relationships with the underlying Bajocian Garantiana Clay Member and the Berreraig Sandstone Formation and the overlying Callovian Staffin Bay Formation constrain the age range for these rocks to latest Bajocian to Bathonian [2, 30–32]. The best exposures of the Great Estuarine Group are on the Isle of Skye, the largest island of the Inner Hebrides. Both new tracksites (BP1 and BP3) are located at Brothers' Point on the Trotternish Peninsula and occur in the Lonfearn Member of the Lealt Shale Formation (Great Estuarine Group).

BP1 is located on an inter-tidal platform east of the mouth of Lonfearn Burn and immediately adjacent to the large sill that forms the western edge of Sgeir Gharbh (57.5865° N, 6.1472° W; Fig 1B). This sill is referred to as the Burn Mouth Sill (John Hudson, personal communication). The walking path to Brothers' Point passes along the cliff face to the south of the outcrop and a small stream branches off from Lonfearn Burn and flows along the western side of the platform. BP1 is regularly exposed during low tide, although it is frequently covered by seaweed.

BP3 is located immediately west of the mouth of Lonfearn Burn into Port Earlish and south of (shoreward from) a large volcanic intrusion (57.5863° N, 6.1494° W; Fig 1B). The site is found among the large, wave-washed boulders of the coast. Since there was very little growth of seaweed and other coastal life on the exposed surfaces at the time of its discovery in 2017, BP3 likely was covered by boulders until soon before its discovery. Thus, in the future, BP3 may be particularly liable to becoming re-covered during storms.

BP1 and BP3 are located in the upper part of the Lonfearn Member, within the transitional facies between a lagoon-dominated depositional environment and the overlying deltaic sandstones of the Valtos Formation [2].

### Brothers' point 1

The tracks at BP1 are preserved as impressions (concave epirelief) in a dark gray, thinly-laminated, fine-grained calcareous shale overlain and in-filled by a light tan, bioclastic limestone. Upon close examination, the track-bearing horizon is composed predominantly of clay to silt-sized carbonate mud with intermittent, weakly defined layers of broken bivalve shells. Moderate pyritization occurs around the outer edges of some of the larger shells in the section.

The shale of the track-bearing layer contains extensive mudcracks that often propagate from the toes of the tridactyl tracks. This association of mudcracks and dinosaur tracks indicates that both features were formed near the same time when the sediments in question were exposed subaerially. Fig 1C shows a stratigraphic section of BP1 through the beds immediately above and below the track-bearing layer. The section is dominated by shales with isolated beds of coarser shelly limestones and sandstones. The track-bearing layer marks the only definitive subaerial exposure in this short (1.90 m) section that was logged at the cm-scale. In some beds below the track-bearing layer, broken bivalve shells are visible to the naked eye and lend support to the inference that the area was generally subaqueous. Additionally, the lithology immediately above the track-bearing layer indicates the subaerial exposure observed at the site was rather transient. In particular, the presence of a thin bone bed comprised of broken fish material immediately above the bioclastic limestone that infills the tracks provides strong evidence that the site was resubmerged after the desiccation event in which the mudcracks formed.

The limestone unit overlying the track-bearing layer is composed almost exclusively of densely packed shells of the bivalve *Neomiodon* (John Hudson, personal communication). Monotypic shells beds such as these are characteristic of the upper portions of the Lealt Shale Formation's Lonfearn Member [2, 33]. In addition to *Neomiodon* as the dominant invertebrate, isolated smooth-shelled ostracods, possibly *Alicenula phaselus*, are present (Matt Wakefield, personal communication). Very rarely, broken gastropods are visible in thin section.

One of the characteristics of a brackish-water faunal assemblage is a low variety of species and a large number of individuals [33]. The assemblage of predominantly *Neomiodon*, with lower concentrations of *Viviparus*, ostracods and conchostracans (known in older literature as *Estheria*, *Euestheria*, *Cyzicus*, and spinicaudatans) is indicative of a low-salinity environment [33]. This faunal assemblage indicates that the track-bearing bed and adjacent layers are

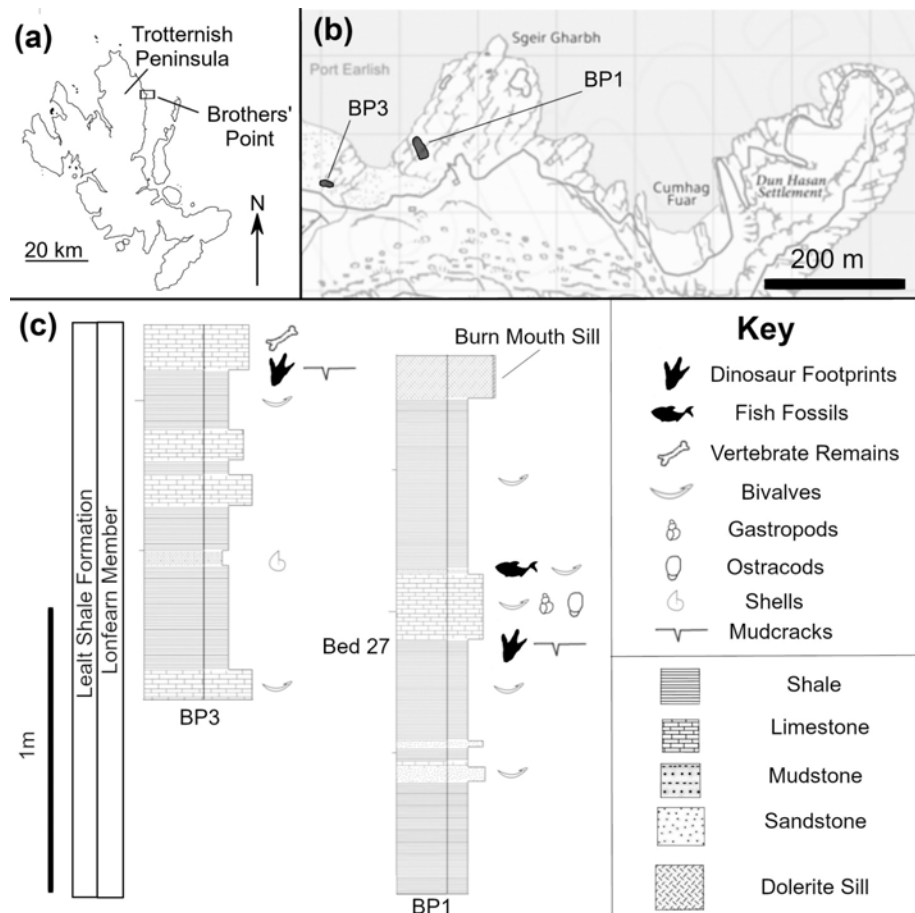


**Fig 1. Geographical and geological context of BP1 and BP3.** The geographical location of the sites on (a) the Isle of Skye and (b) the Trotternish Peninsula and (c) the bedding-scale stratigraphy of the Lonfearn Member, Lealt Shale Formation around each site. Bed 27 marks the inferred stratigraphic layer of the first dinosaur footprint from Scotland [22] according to the numbering scheme from [2]. It is located at or near the level of the track-bearing layer at BP1. Maps adapted from BGS 1:50 000 [Shapefile geospatial data], scale 1:50 000, tile: SC0803, version 2016, British Geological Survey, UK, using: EDINA Geology Digimap Service <http://digimap.edina.ac.uk>, downloaded October 2017, © Geological Map Data BGS © NERC 2017.

<https://doi.org/10.1371/journal.pone.0229640.g001>

located in the transitional zone between the more brackish Lealt Shale Formation and the freshwater Valtos Formation [34].

We reconstruct the depositional environment for BP1 as a briefly exposed, subaerial mud-flat adjacent to brackish (but tending towards freshwater) lagoons. While the dinosaur tracks were made upon a desiccating surface, this time of exposure was, likely, relatively brief in terms of geologic time and, as evidenced by the presence of fish bones in the beds immediately overlying the desiccation surface, the spot was quickly reclaimed by water. The overall environment reconstructed for this area is a dynamic, rapidly fluctuating, coastal margin.

### Brothers' point 3

The tracks at BP3 are preserved as impressions (concave epirelief) in a shale overlain and infilled by a well-sorted, bioclastic limestone (Fig 1C). The shale is medium to dark blue-gray, micritic, and dominated by thin (< 5 mm) laminations. Thin lenses (< 1 mm thick) of a paler colored fine-grained sand are sparsely interspersed between the shale layers. The overlying

bioclastic limestone is predominantly composed of disarticulated to broken shell fragments of *Neomiodon* with mm-scale lenses of dark-colored silt. Large (3–4 mm), subhedral pyrite crystals are present in the bioclastic limestone. They are probably of diagenetic origin [35].

The invertebrate fauna at BP3 is dominated by *Neomiodon*. However, the shell beds are not as densely packed as those at BP1 and mud separates the disarticulated valves. Other invertebrates present at the site include ostracods and conchostracans. Conchostracans are common in the Lealt Shale Formation but become rarer with increasing stratigraphic height within the formation and through the associated facies shift to the Valtos Formation which contains few examples of these invertebrates [2, 36]. Their abundance in the track-bearing mudstone, in particular, is reasonable evidence that the bed in question is still part of the Lealt Shale Formation.

The dinosaur tracks at BP3 occur in a single, track-bearing layer with localized soft-sediment deformation associated with tracks disrupting the underlying thin shaley laminations. Desiccation cracks are not visible along the southern portion of the platform where the largest concentration of tracks is located. However, these sedimentary structures are visible on the same bedding surface about 5 m to the north and are associated with two additional tracks. The variable association of footprint and desiccation crack occurrences can arise due to variations in surface saturation or in the rates at which different portions of the surface dried. Due to the presence of desiccation cracks and the undeformed nature of the overlying bioclastic limestone that is infilling the tracks, it is likely that the currently exposed surface was close to the original surface on which the dinosaurs walked and that it was subaerially exposed near the time of track formation.

While the dinosaur tracks at BP3 were being described, an articulated pterosaur skeleton (illustrated as ‘vertebrate remains’ in Fig 1C) was found in the overlying limestone layer by Amelia Penny. The unfractured nature of the delicate bones (many of which are hollow) and overall completeness of the skeleton indicates that the overlying limestone was deposited in a relatively low-energy environment. This specimen is currently under study and will be fully described in a subsequent PalAlba publication. The inferred energy setting of the overlying limestone indicates that, when the track-bearing surface was resubmerged, the influence of currents, tides, and other potential mechanisms for reworking material was relatively minimal. Thus, the subsequent environment supported the preservation of these tracks.

We interpret the depositional environment for BP3, like at BP1, as a briefly exposed, sub-aerial mudflat where the dinosaur tracks were formed on a desiccating surface. The area was quickly reclaimed by the adjacent, low-energy, brackish to freshwater lagoons. The depositional environment for BP3 corresponds to that determined for BP1 – a rapidly changing coastal margin.

### Stratigraphic context of the tracksites

Several detailed stratigraphic sections for the Lealt Shale Formation have been published [2,29] and the locations of BP1 and BP3 can be loosely tied into these broader schemes. Bed-by-bed correlation upwards from the stratigraphically lower ‘6 m Sill’ several hundred meters to the east and bedding-scale sedimentological observations support the inference that BP1 is located in or near ‘Bed 27’ of the Lonfearn Member (Lealt Shale Formation; numbering from [2]). BP3 seems to be located slightly higher in the section based the dominant dip of the stratigraphy (~5–8°, dip direction = ~345°) and its geographic location relative to BP1. The precise stratigraphic position of BP3, relative to BP1, is particularly difficult to determine with confidence due to localized metamorphism, poor exposure of the sedimentary layers along the rocky

shoreline, and possible faulting across Lonfearn Burn (John Hudson, personal communication).

These correlations are notable because Bed 27 is the inferred source of the first dinosaur fossil ever discovered on Skye (and indeed, in Scotland): the single footprint (GLAHM V1980), mentioned above, preserved as a positive relief cast (convex hyporelief) on a loose block that had fallen from a cliff further south at Brothers' Point (~500–600 meters away) [22]. Thus, it is likely that both BP1 and BP3 are closely located stratigraphically to the rocks from which this original footprint derived. It may be possible that one or more of these beds preserve extensive tracksite surfaces across hundreds of meters of lateral continuity, but which are not discernable at outcrop scale because of the patchy nature of the exposures and the extensive metamorphism around Brothers' Point. Indeed, other track-bearing surfaces appear slightly lower in the section at Brothers' Point Site 2 which is located immediately above the '6 m sill' in Beds 24 and 25 [25].

## Materials and methods

### Sampling permissions and ethics statement

Permission to conduct the study and collect drone-based data was granted by Scottish National Heritage (SNH). No plant or animal material was collected in this study.

### Track descriptions and measurements overview

The vast majority of the tracks at BP1/BP3 retain infillings or drapes of the overlying sedimentary unit. Although seaweed and some of the encrusting limpets were removed from the track surfaces, the tracks were not prepared further (i.e. the infilling-sediment was not removed) in the context of this study. The qualitative terminology used to describe these tracks follows the definitions found in [37, 38]. Additionally, each track was assigned a numerical value to quantify the quality of preservation according to the scheme of [39] (recently expanded by [40]). These numerical grades (S1 Appendix of S1 Table) allow appropriate caution to be exercised in making ichnotaxonomic assignments and help ensure track comparisons are made between specimens with similar levels of preservation.

Both tracksites are located on active modern tidal platforms. Therefore, the tracks can be measured only during the low tide window. Due to this time constraint, we took summary measurements (track length and track width) in the field while all other measurements were either taken from field photographs using ImageJ 1.51k [41] or from the scaled photogrammetric models of the sites using CloudCompare v2.8.

**Tridactyl and quadrupedal tracks.** We collected the following measurements for tridactyl tracks: total track length (L), total track width (W), total digital length (LII and LIV), basal digital length (BL), basal digital width (WB), middle digital width (WM), the heel-interdigital (hypex) distances (K and M), and the interdigital angles between digits II-III and digits III-IV ( $\alpha, \beta$ ) (Fig 2). We also noted several additional qualitative features including the presence or absence of claws on the digits, the presence or absence of pads on the digits, the shape of the digits, and the shape of the 'heel' [42, 43].

We measured the manus and pes of quadrupedal tracks with length and width measurements as detailed by [44, 45] (Fig 3). Additionally, we made note of qualitative features like sediment displacement rims, heel marks, and the shape and extent of the digits.

We divided tracks into size classes using the general criteria outlined in [44] for sauropods and bipedal dinosaurs (ornithopods and theropods) and expanded upon by [46] for thyrocephorans (S1 Appendix of S2 Table).

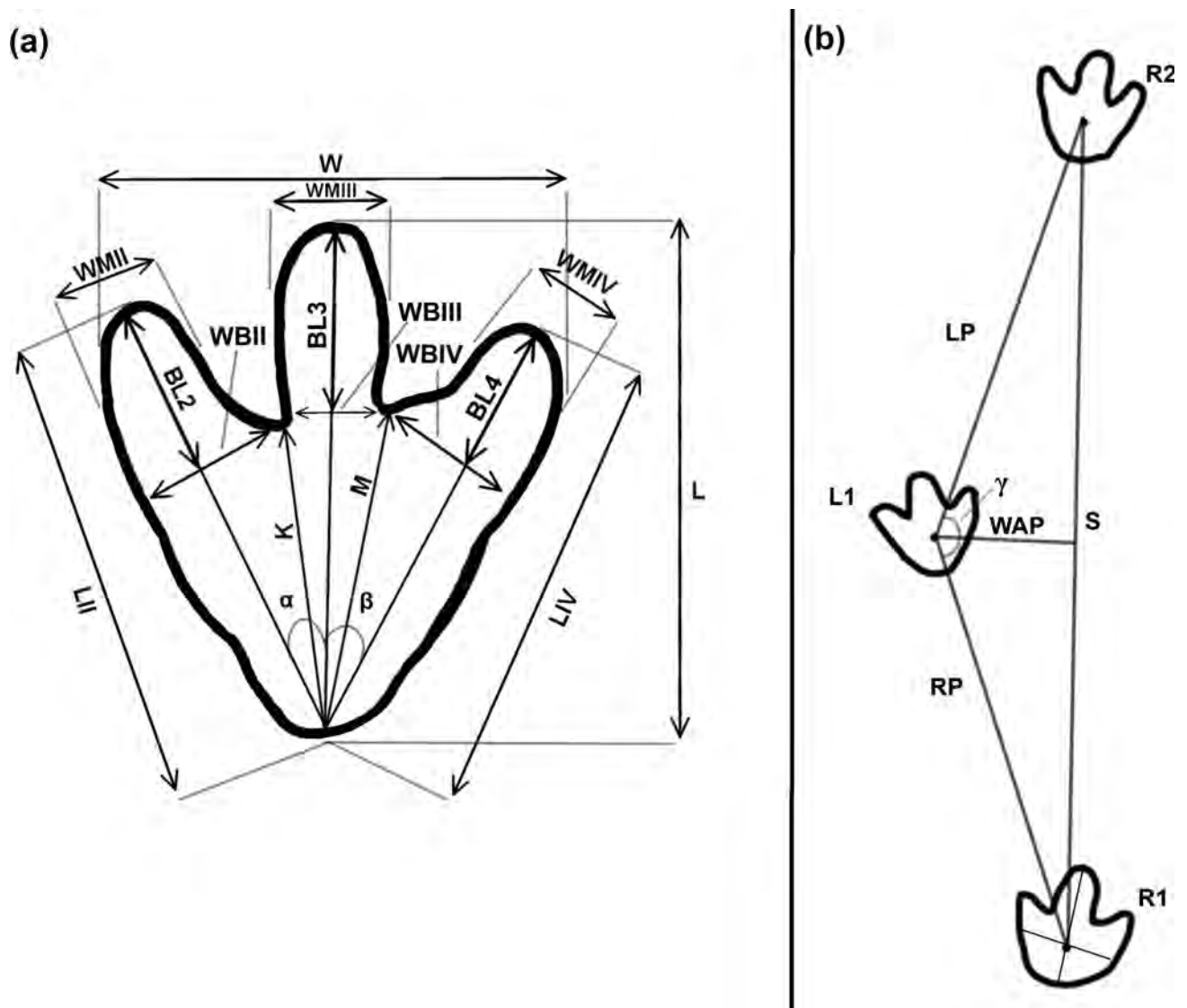


**Fig 2. Track measurements for tridactyl tracks and trackways.** (a) The measurements taken for each tridactyl track were derived from [37, 38, 42]. The abbreviations on the figure are as follows: total track length (L), total track width (W), total digital length (LII and LIV), basal digital length (BL), basal digital width (WB), middle digital width (WM), the heel-interdigital (hypex) distances (K and M), and the interdigital angles between digits II-III and digits III-IV ( $\alpha$ ,  $\beta$ ). (b) This simplified bipedal tridactyl trackway shows how left and right pace (LP, RP), stride (S), width of angulation pattern (WAP), and the pace angulation ( $\gamma$ ) are measured. Additionally, the lines used to define the ‘center of the track’ for trackway measurements are illustrated on track R1.

<https://doi.org/10.1371/journal.pone.0229640.g002>

**Trackway measurements.** We described bipedal trackways using pace (P), stride (S), width of angulation pattern (WAP), angle of rotation ( $\alpha$ ), and pace angulation ( $\gamma$ ). Fig 2B shows an idealized approach to taking bipedal trackway measurements [44, 47, 48]. The pace of a bipedal trackway is the distance between consecutive, alternating footprints (i.e. right-left or left-right) [49]. Stride length is defined as the distance between corresponding points in successive prints from the same foot (i.e. the distance between one right pes impression and the next) [37, 38]. [38] suggested that the best reference point for bipedal trackway measurements is the “tip of the principal digit” as it is often a well-defined feature. Later workers have broadly adopted this practice using the tip of digit III as the point of reference [44, 50]. This approach,

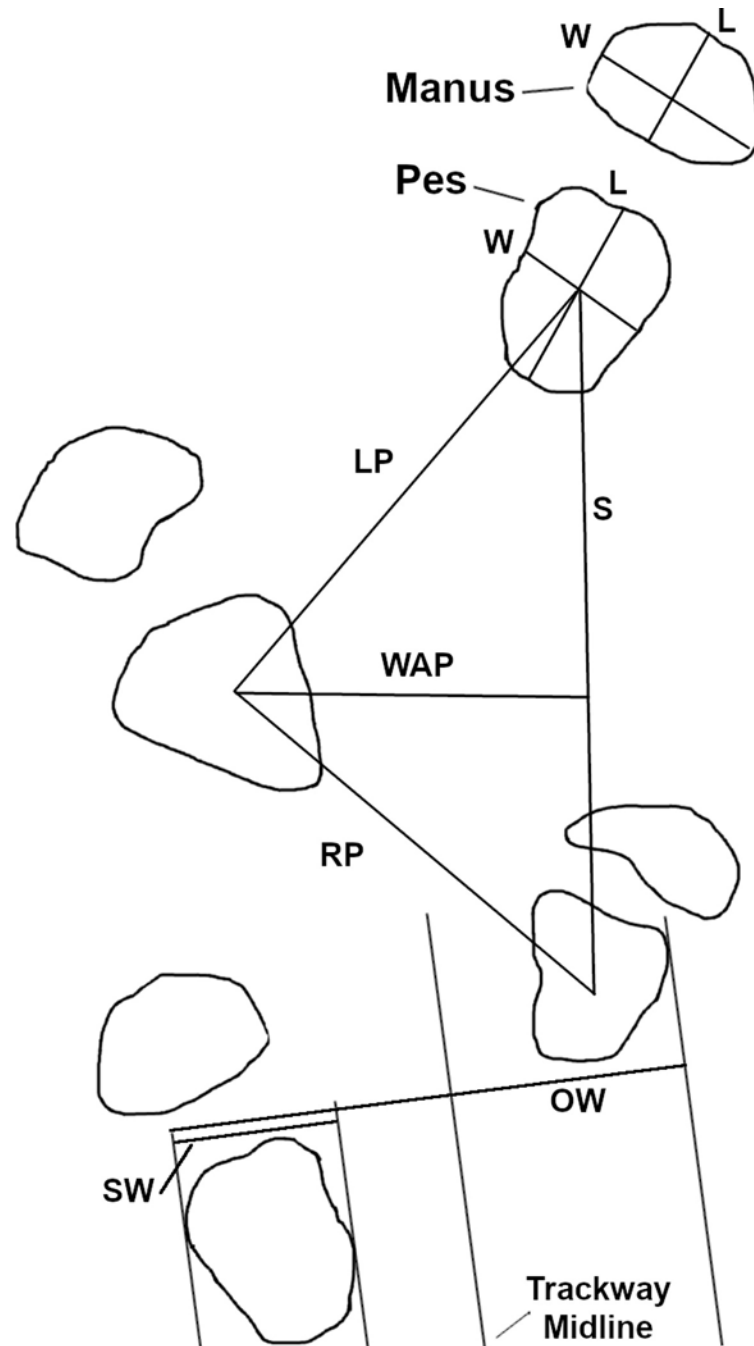


**Fig 3. Quadrupedal track and trackway measurements.** Length (L) and width (W) show the individual track measurements taken on quadrupedal tracks at Brothers' Point. Trackway characteristics such as the left and right pace (LP, RP), stride (S), width of angulation pattern (WAP), side width (SW) and overall width (OW) were also measured. Figure adapted from [44].

<https://doi.org/10.1371/journal.pone.0229640.g003>

however, proved impractical for the bipedal trackways from Brothers' Point as they are usually short (3–5 tracks) and poorly preserved without consistently distinctive digit impressions. Therefore, we selected points of correspondence for measuring each individual trackway by assessing the common features between the component tracks of the trackway. In practice, the

best correspondence point was defined as the “center of the track” (either the intersection of the axis of digit III and a perpendicular line halfway between the base of digit three and the rearmost portion of the heel or, when the toes or heel were indistinct, the intersection of the long and short track axes).

The width of angulation is a measure of the overall trackway width using established reference points on alternating (right-left) tracks. It can be calculated by applying the Pythagorean Theorem to the pace and stride lengths (*sensu* [44]; Fig 2B). The angle of rotation ( $\alpha$ ) is the angle between the long axis of a track and the midline of the trackway. Pace angulation of a bipedal trackway is measured as the angle between the lines used for two successive pace measurements (e.g. the angle between the right pace and the left pace as shown in Fig 2B) [38, 44, 49].

We applied the measurements used to describe quadrupedal trackways (pace, stride, width of angulation, and progression) to both manus and pes impressions [38, 44]. The pace, stride, and width of angulation of quadrupedal trackways are defined in the same manner as those of bipedal trackways (Fig 3). Progression describes how far forward the trackmaker moved during a single footfall and was calculated using Eq 1, where WAP is the width of the pes angulation pattern [44]. The progression of the trackways was calculated only for the pes impressions, as manus impressions were sparse in the quadrupedal trackway from Brothers' Point.

$$Progression = [(pace)^2 - (WAP)^2]^{(0.5)} \quad (1)$$

The reference point for measurements made between successive quadrupedal tracks is the intersection of the lines along which length and width were measured [37, 38, 44].

Other bipedal and quadrupedal trackway measurements that we took include overall trackway length (measured from the heel of the first impression to the toe of the last) and trackway orientation (measured relative to magnetic north).

In addition to the trackway measures detailed above, we quantified the quadrupedal trackways according to gauge. While sauropod trackways have been divided into 'wide-gauge' and 'narrow-gauge' categories for about a quarter of a century [51], a more quantitative assessment of gauge called the 'track ratio' was recently proposed [52]. The track ratio can be calculated using Eq 2, where SW is the side width of the footprint (the width measured perpendicular to the trackway midline) and OW is the overall width (the width measured from the outermost edges of subsequent right and left impressions perpendicular to the trackway midline) (cf. Fig 3, [52]).

$$Track\ Ratio = \left( \frac{SW}{OW} \right) \times 100\% \quad (2)$$

We used track and trackway measurements to determine the estimated hip height, speed, and gait of the dinosaurian trackmakers. Several different approaches to measuring hip height have been reported in the literature. The most commonly used relationship (Eq 3) correlates footprint length (FL) with hip height ( $h$ ) through a scaling factor [53].

$$h = 4.0 \times FL \quad (3)$$

Computer modeling has demonstrated that this equation provides a good estimation of hip heights of bipedal trackmakers [54] and, thus, makes it a reasonable approximation to use for later calculations.

The most effective way to estimate the size of quadrupedal dinosaurian trackmakers, particularly sauropods, is the topic of on-going debate [55]. Thus, Eq 3 was used for the footprints

from the quadrupedal trackway to provide a first-order estimation of the hip height. In addition to this estimation, a thyreophoran hip height formula (Eq 4) developed by examining the skeletal proportions of *Kentrosaurus* was used to estimate the hip height ( $h$ ) of the quadrupedal trackmakers from the width of the pes ( $W$ ) [56].

$$h = 6 W \quad (4)$$

The speed at which a dinosaur was traveling while leaving a trackway can be approximated with the following empirical equation (Eq 5), where  $v$  represents the speed in meters per second,  $g$  is the gravitational constant ( $9.81 \text{ m/s}^2$ ),  $S$  is the stride length of the trackway (m), and  $h$  is hip height (m) [53]. This equation most appropriately applies to trackways left by the animals moving at walking pace (denoted as where the  $S/h$  ratio is less than 2.0) [44].

$$v \approx 0.25g^{0.5}S^{1.67}h^{-1.17} \quad (5)$$

Estimating the speed at which a dinosaur was traveling relies on several assumptions with large amounts of uncertainty. One, in particular, is that the empirical relationships derived from mammal measurements can be extended to dinosaurs and the assumption that foot length is a reasonable proxy for hip height. With that said, the estimates provide a general predictor of speed that is consistent with other biomechanical considerations [57]. Essentially, the uncertainty inherent in determining the speed of dinosaurs must be acknowledged and the results of such calculations regarded as broad estimations rather than strict answers.

The gait of a dinosaur can be qualitatively described as walking, trotting, and running [58]. The points at which an animal transitions between gaits can roughly be defined using the relationship between stride length ( $S$ ) and hip height ( $h$ ). The relationship, walking  $< 2.0 <$  trotting  $< 2.9 <$  running, denotes what values of  $S/h$  approximate each gait [58].

Broad observations about the rate at which the trackway makers were moving through their respective environments can be made using these relationships. These observations can then support behavioral inferences.

*Ambiguity in tridactyl trackmakers and puzzles of preservation.* A common goal of track analysis is identifying the most likely trackmaking organisms. However, the overall shape of a track is influenced by some combination of three factors—autopodial anatomy (the shape of the foot), its dynamic motion (how the animal is locomoting), and the conditions of the substrate across which it traverses [59]. Frustratingly, the combination of these factors implies both that a single trackmaking organism can produce a variety of different track morphologies (as seen in the case of individual trackways in [60]) or different organisms can produce similar track morphologies. Additionally, the shape of a track can be further influenced by post-registrational taphonomic processes (those that occur after the autopodium has ceased contact with the substrate) like the desiccation of the trackbearing surface preburial or modern erosion [40].

In the case of footprints attributed to dinosaurs, tridactyl tracks prove particularly challenging to reliably assign to definitive trackmakers. Tridactyl tracks are commonly attributed to two clades of dinosaurian trackmakers—theropods and ornithopods—and discriminating between these trackmakers has historically been and continues to be a challenge [42, 61, 62]. The challenge of differentiating between these trackmakers arises because both dinosaur clades possess a functionally tridactyl, mesaxonic pes [63].

Some qualitative parameters including the length/width ratio, shape and length of the toes, presence or absence of claw impressions, and shape of the ‘heel’ have been traditionally used to distinguish between theropod and ornithopod trackmakers [38, 49]. Over the last thirty years,

multivariate analyses of linear track parameters and ratios have also seen use in differentiating between theropod and ornithopod footprints [42, 61, 64, 65] and, more recently, geometric morphometric analyses have been brought to bear to investigate the question [62, 66].

However, both the qualitative and quantitative parameters are reliant on assessing a reasonable outline of the footprint in question. This process has been demonstrated to be subjective to the observer as the shape of a footprint and its resultant linear measurements can vary radically based on where and how the track outline is defined [67]. [67] recommends the most objective way to determine the shape of the track is to specify minimum (where the track walls meet the track floor) and maximum outlines (where the track intersects with the tracking surface) to 'bracket' the variations within the shape of a single track. In the case of the Brothers' Point tracks, applying this method is not feasible for many tracks because of the presence of sedimentary infills which obscure both the track walls and the track floor. The 2d track outlines of these tracks generally follow the contact between the infilling sedimentary material and the plane of the trackbearing surface (excluding clear displacement rims or additional soft sediment deformation). These sedimentary infills also make observation of features associated with the track floor impossible and potentially could distort or disturb the original shape of the track impression.

When it comes to the footprints at Brothers' Point, three main post-registrational taphonomic processes negatively affect the morphological preservation of the tracks—the propagation of cross-cutting dessication cracks from the impressions as the track-bearing surface dries, the subsequent infilling of the impressions by sediment, and erosion from the highly energetic modern tidal environment in which the tracks are exposed [40]. The consistently low preservation grade of the footprints and widespread occurrence of infilling sediments across the two tracksites calls into question the reliability of track shapes reconstructed and, in particular, raises the specter of linear measurements in the study being strongly affected by biases in morphological preservation [40, 67]. In particular, the lengths of the digits and the placement of track hypices are strongly affected by both the depth at which they are measured within the track and by sedimentary infilling [67]. Recognizing these limitations, we refrain from definitively assigning any tridactyl footprints in this study to ichnotaxa. Furthermore, although the likelihood parameters developed in [42] are used to investigate additional lines of evidence for either theropod or ornithopod affinities, the results of such ratios are not relied upon for definitive differentiation between dinosaur clades and instead are used to spur further reflection on possible trackmaker affinities. Thus, although both qualitative and quantitative parameters are used to investigate the likelihood of theropod and ornithopod trackmakers at the sites, the limitations of the footprints at these sites means that clear, unequivocal discrimination between these dinosaur groups is not possible. This uncertainty makes subsequent interpretations of different bipedal dinosaurian trackmakers somewhat speculative.

*Photogrammetric models: Data capture and construction.* Recently, unmanned aerial vehicles (UAVs, a.k.a. drones) have been used by paleontologists to document difficult trackway exposures [68–71]. Digital models (e.g. photogrammetric, LiDAR) of tracksites preserve spatial relationships between footprints over large areas and can provide lasting documentation of sites that are particularly susceptible to erosion or that are only exposed for a short time as the result of construction or mining activities [44, 71, 72]. At Brothers' Point, we sought to automate the process of collecting the photographs for photogrammetric models because of the moderately expansive lateral extent and tidal nature of the tracksites.

At BP1, we used a custom UAV hexacopter built around a Tarot 680 Pro airframe with a payload of a Sony A6000 (24 mp, 20 mm lens) camera oriented at nadir. The Sony A6000 camera was run in aperture priority mode using an external trigger from the flight controller of the UAV. A total of 7 flights were completed over the exposure at varying heights above the

ground surface (3 m and 6 m). The UAV was flown along a parallel survey line pattern using Pixhawk flight controllers running Arducopter 3.3 firmware and was operated from a ground control station running Mission Planner v.1.3.41 and communicating with the aircraft over a 433 MHz telemetry link. The flight paths and triggering locations for the aircraft were calculated in Mission Planner prior to the flights and the aircraft were operated in autonomous mode to ensure adequate photo coverage for later photogrammetric work. Twenty-four ground control points (GCPs) were included in the survey. Several markers were placed immediately outside the region of interest while others were spaced 'randomly' across the track platform itself. Using preexisting fractures was preferable to hammering directly into the rock, so we preferentially placed the GCP markers within these structures on the outcrop.

The unpredictability of the weather on Skye meant that the drone could not easily be flown at all the tracksites. Thus, to map BP3, we constructed an intervalometer to substitute for the drone. The intervalometer combined principles of time-lapse photography with a paired set of overlapping cameras arranged on a pole to collect a photogrammetric dataset with enough end lap and side lap for model construction. The cameras used to construct the intervalometer were Canon S110 (12 mp). The Canon S110 cameras were modified using CHDK (Canon Hacker Development Kit) firmware to enable external triggering of the camera and greater control of the ISO, aperture, and shutter speed. [S1 Appendix](#) contains further details of the intervalometer design and an assessment of its utility. Four GCPs were included in the survey. A similar approach to GCP distribution to BP1 was employed at BP3.

We used relative carrier phase GNSS (Global Navigation Satellite System) data collected using Leica GS10 receivers as GCPs to constrain the photogrammetric models of BP1. On the day of the GNSS survey, a base station was established at the site and allowed to collect location data for 4–5 hours. Individual ground control points on the outcrop were captured using a roving receiver mounted on a bipod-supported pole. The roving receiver remained at each ground control point for approximately five minutes. The ground control points were then paired with the base station to resolve ambiguities and perform an initial quality control check.

We used relative carrier phase GNSS (Global Navigation Satellite System) data collected using Leica SR530 receivers operating in RTK (real-time kinematic) mode as GCPs to constrain the photogrammetric model of BP3. On the day of the GNSS survey, a base station was established at the site and allowed to collect location data for ~3 hours. Individual ground control points on the outcrop were captured using a roving receiver mounted on a pole. Final control point locations were averaged from five field measurements of the location.

In both cases, the cut-off angle for satellites surveyed was 10° above the horizon. Upon returning from the field, the base stations were paired to an established Ordnance Survey reference station. The reference station used (Lochcarron–LCAR) was 44 km from Brothers' Point.

The GNSS survey of BP1 was refined with precise ephemeris data downloaded from the International GNSS Service (IGS) ([https://igsceb.jpl.nasa.gov/components/prods\\_cb.html](https://igsceb.jpl.nasa.gov/components/prods_cb.html)) on April 10, 2017. The estimated position quality for the ground control points was ~1 cm. Precise ephemeris data were not used to refine the results of the GNSS survey of BP3 because the potential location improvements were negligible given the length of the baseline, meaning the quality of the survey would not have been significantly improved. The estimated position quality for the ground control points was ~1 cm for both sites.

We generated a photogrammetric model of each tracksite in Agisoft Photoscan 1.2.5.2735 on the SAMSON workstation of the Airborne Geosciences Facility at the University of Edinburgh. A total of 284 images (from a drone flown at approximately 3 m above the ground surface) were used to construct the tracksite model of BP1. The Ground Sampling Resolution of the generated orthophoto was 0.6 mm/pix. The calculated error for the control points within the model averaged to 7.00 cm with 3.58 cm averaged error for the checkpoints. 460 images

(from an intervalometer held approximately 1.5 m above the ground surface) were used to construct the tracksite model of BP3. The Ground Sampling Resolution of the generated orthophoto was 0.3 mm/pix. The calculated error for the control points within the model ranged between 1.74 cm and 6.17 cm for the checkpoints. The model processing protocol both models can be found in [S1 Appendix](#). Links to the photosets used to construct BP1 and BP3 can be found in [S1 Appendix](#).

The accuracy of the models was further evaluated by comparing measurements made in model space with field measurements. The >0.99 correlation coefficient between the field data and the model data yielded for both tracksites indicates that measurements taken from the site models and orthophotos can be considered representative of the reality of the track-bearing surface ([S1 Appendix](#) of Fig 6).

### Site overviews

We generated photogrammetric models and orthophotos for both tracksites. A link to high-quality versions of all orthophotos and models is in the [S1 Appendix](#).

Thirty-five individual tracks (labeled BP1\_01 –BP1\_35) were identified at BP1. There are three distinctive trackways (in-text labels BP1\_Twy\_01 –BP1\_Twy\_03), a track association (TA\_1), and a range of isolated tracks of varying quality. The orthophoto generated from the photogrammetric model ([Fig 4A](#) and [S1 Appendix](#)) was used as the base for the site map ([Fig 4B](#)).

Eighteen tracks were identified at BP3 with sixteen located in the area surveyed for photogrammetric modeling. The tracksite encompasses two bipedal trackways (BP3\_Twy\_01 and BP3\_Twy\_02) and a scattering of isolated tracks at varying orientations. The orthophoto generated from the photogrammetric model ([Fig 5A](#) and [S1 Appendix](#)) was used as the base for the site map ([Fig 5B](#)). After the photogrammetric survey was complete, two additional tracks were found in a second exposure of the track-bearing layer approximately 5 m northeast of the main platform. These tracks were mapped separately from the main track grouping at BP3 ([Fig 5C](#)).

### Track descriptions and ichnotaxonomy

Comprehensive lists of track measurements and observations for both BP1 and BP3 that are not discussed in-text can be found in [S1 Appendix](#).

#### Brothers' point 1

A variety of track morphologies are preserved at Brothers' Point 1, including broken casts, several different types of tridactyl footprints, and sub-circular to ovoid tracks that comprise a quadrupedal trackway. Overall, three trackways are observable: the quadrupedal sequence (BP1\_Twy\_01) and two bipedal ones (BP1\_Twy\_02 –BP1\_Twy\_03). The 35 total tracks observed at the site are numbered using a system of BP1\_01, BP1\_02, etc.

**Quadrupedal trackway (BP1\_Twy\_01).** Of particular interest among the tracks at the site is a single, short quadrupedal trackway (BP1\_Twy\_01) that crosses the northern edge of the platform before passing underneath the overlying limestone layer ([Fig 4](#)). The trackway ([Fig 6](#)) consists of five definitive and two additional possible tracks located out of the expected line of trackway progression. [S1 Appendix](#) has a link to a subsample of the outcrop model focused on this trackway.

Using the schema outlined in [39, 40], the preservation grade of the tracks in BP1\_Twy\_01 is 1 because the manus can be distinguished from the pes, there are the remnants of toe marks, and the general outline of the footprints is preserved, but there are not clear indications of

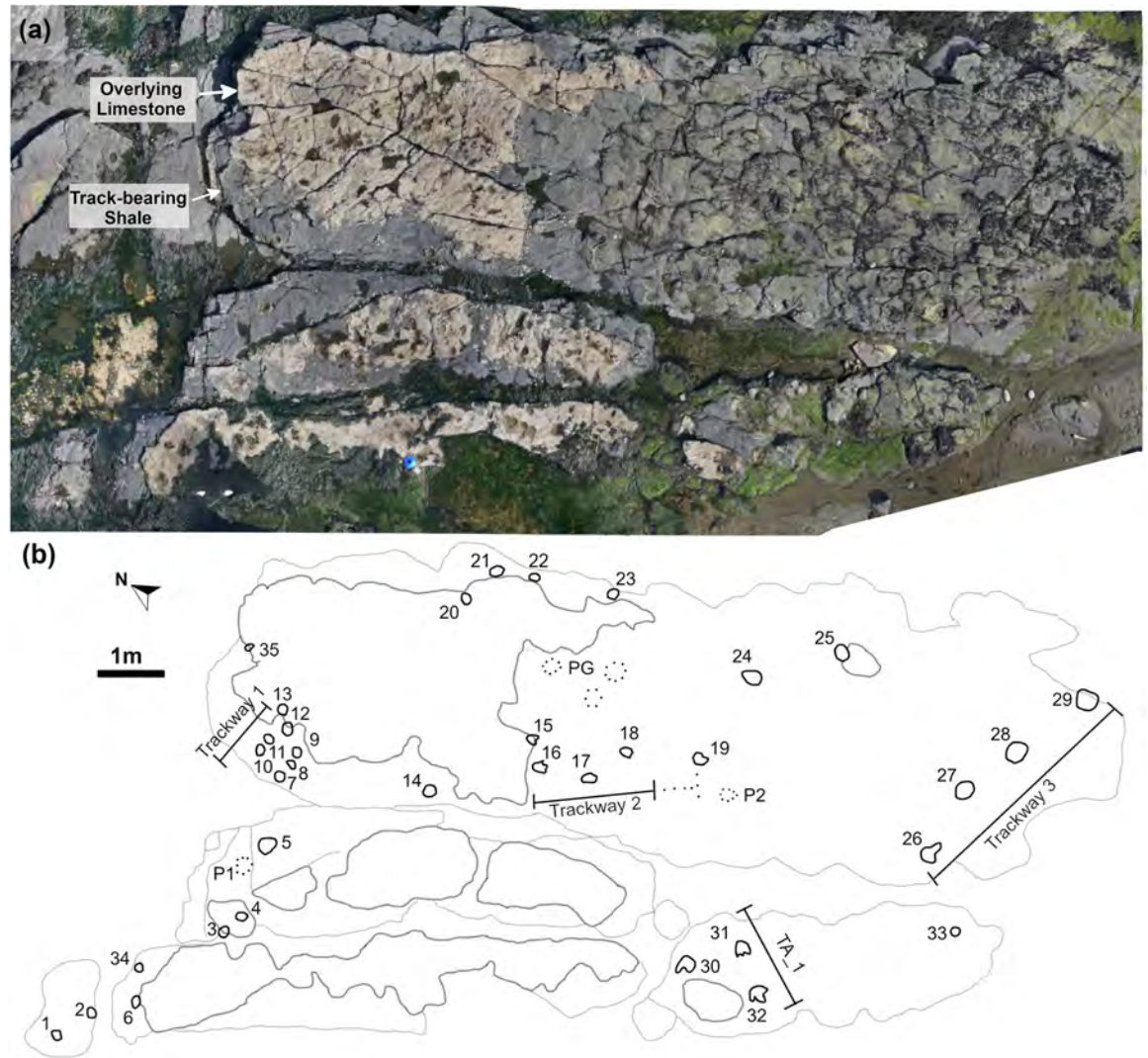


**Fig 4. Orthophoto and site map of BP1.** (a) The orthophoto for Brother's Point Site 1 (BP1) strikingly demonstrates the high contrast between the dark gray, track-bearing shale and the overlying and in-filling light tan limestone in the Lonfearn Member of the Lealt Shale Formation. (b) The site map highlights the track distribution spatially and denotes the orientation and length of the trackways relative to one another. Each individual track is labeled with its field number (1–35). P1 and P2 denote 'possible' tracks 1 and 2 while PG denotes a 'possible group' of shallow impressions. Thick black lines denote the track outlines while lighter lines highlight the contrast between the lithologies and fractures on the outcrop. Dark gray lines delineate the extent of the limestone while lighter gray lines show the platform edges of the shale and some fractures within it. One quadrupedal trackway (Trackway 1; BP1\_Twy\_01), two bipedal trackways (Trackway 2–3; BP1\_Twy\_02–BP1\_Twy\_03), and one set of associated tracks (TA\_1) are present at the site.

<https://doi.org/10.1371/journal.pone.0229640.g004>

ungual marks or digital pads. The manus tracks are crescent-shaped with a convex anterior margin and a less curved posterior margin. The inner edge of the manus tracks has a subtle protrusion on it (Fig 7). Although this protrusion could be the result of the animal's locomotion, the structure of the manus potentially played a greater role in the formation of this feature. This conclusion is suggested by a relatively low amount of soft-sediment deformation immediately adjacent to the protrusion. This protrusion is possibly the remnant of a pollex impression and makes the manus weakly entaxonic. The average manus length is ~10 cm and width is ~15 cm which yields an average L/W ratio of 1:1.5. The pes tracks are tridactyl with weak indications of short blunt toes along the anterior margin. Digit III is slightly more well-

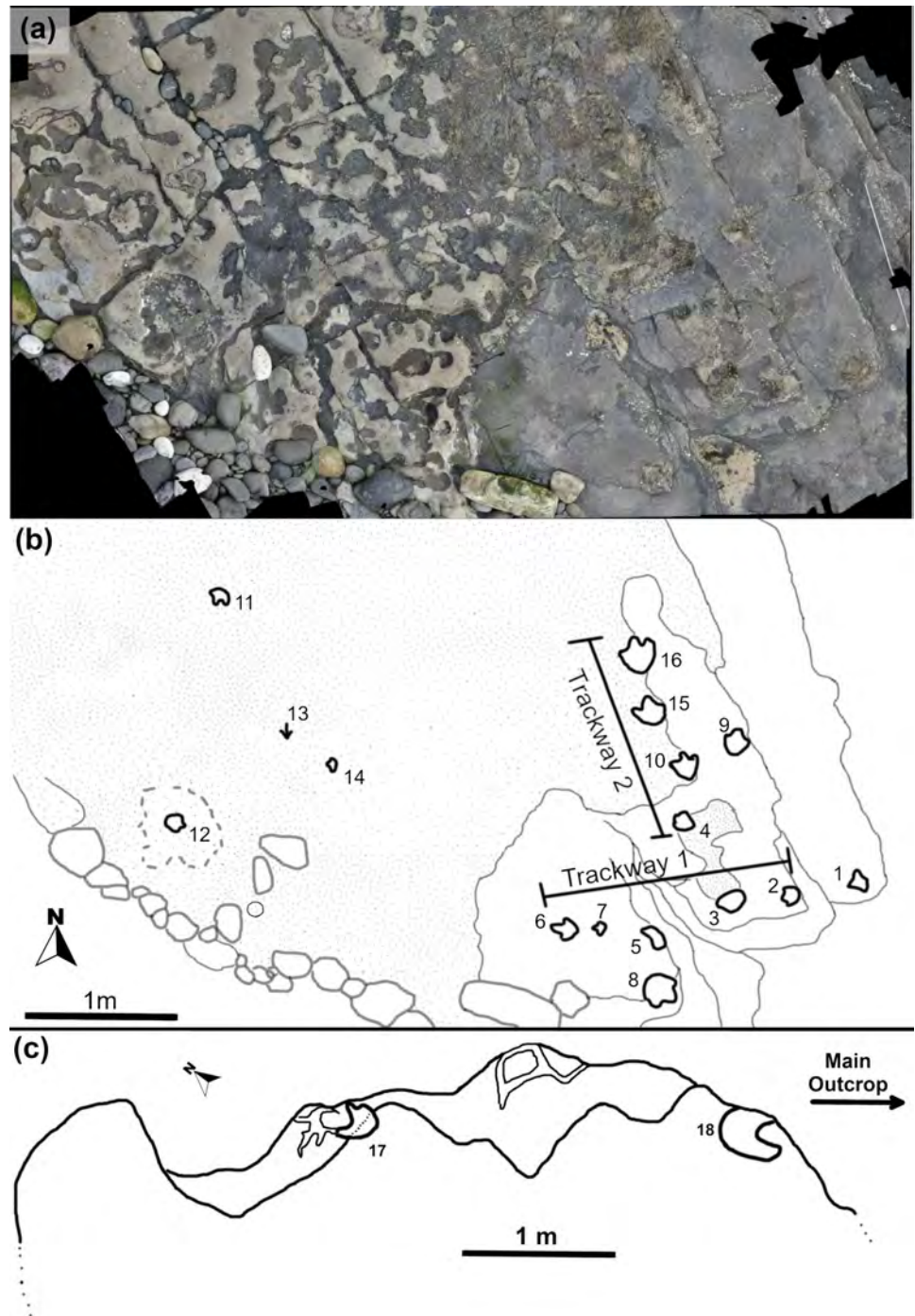


**Fig 5. Orthophoto and site map of BP3.** (a) The photogrammetric orthophoto of BP3 is oriented relative to geographic north. In this image, the largest concentration of tracks occurs in the southeast corner (lower left). Large tracks can be recognized as tan to gray disturbances in the otherwise smooth surface of the outcrop. (b) Line drawing of the site emphasizing both the locations of individual tracks (labeled with their field numbers; 1–16) and the path which trackways take (with Trackway 1–2 corresponding to BP3\_Twy\_01–02). The overlying limestone is denoted with light stippling. (c) The small extension of the main bedding plane of the track-bearing layer at BP3 is approximately 5 m to the north. Extensive mudcracks are present on the surface with some of the most prominent ones propagating from the toes of the two tridactyl tracks (17 and 18).

<https://doi.org/10.1371/journal.pone.0229640.g005>

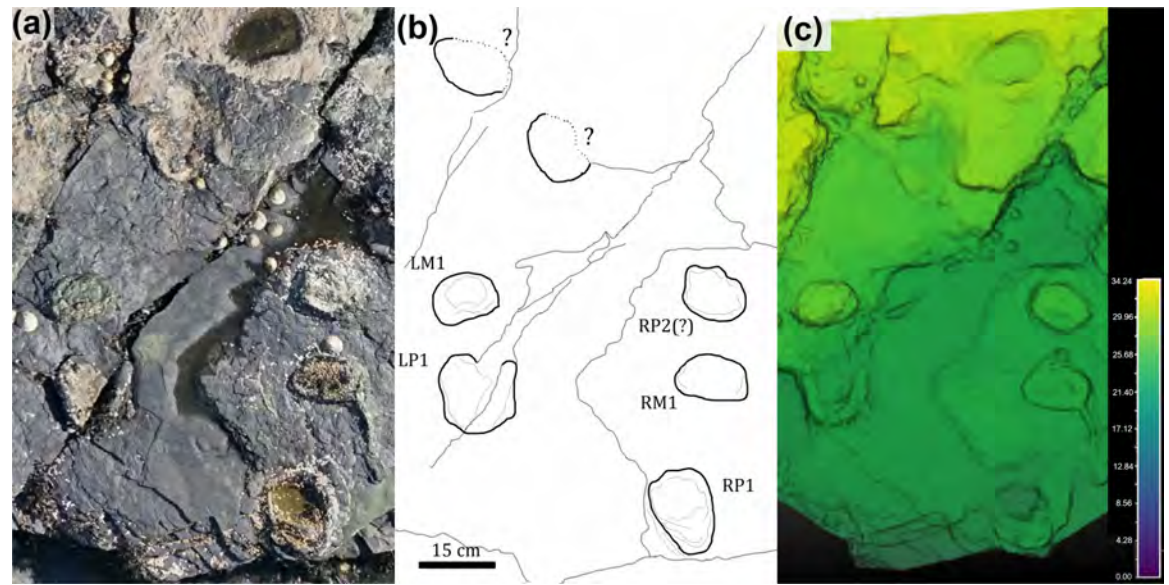


**Fig 6. Quadrupedal trackway (BP1\_Twy\_01) at BP1.** The quadrupedal trackway (BP1\_Twy\_01) shown in an (a) orthophoto from the tracksite photogrammetric model, (b) a line drawing emphasizing distinctive track features, and (c) a false color depth map rendered from the photogrammetric model. Five tracks are clearly associated into the trackway and represent alternating steps with the right manus/pes pair (RM1/RP1) and the left manus/ pes pair (LM1/LP1). Two additional tracks occur immediately above the trackway. However, they are out of line with the trackway progression and their edges are largely obscured by the overlying, light tan limestone layer. Thus, the trackway association is less clear. The color scale of (c) is in units of cm.

<https://doi.org/10.1371/journal.pone.0229640.g006>

defined than digits II and IV. The pes tracks are weakly mesaxonic, elongate, suboval to sub-triangular, and widen anteriorly. The medial and lateral margins of the pes are both nearly straight and the widest point of the pes is located near its anterior margin. The average pes length is ~17 cm and the average width is ~12 cm which yields an average L/W ratio of 1:0.71.

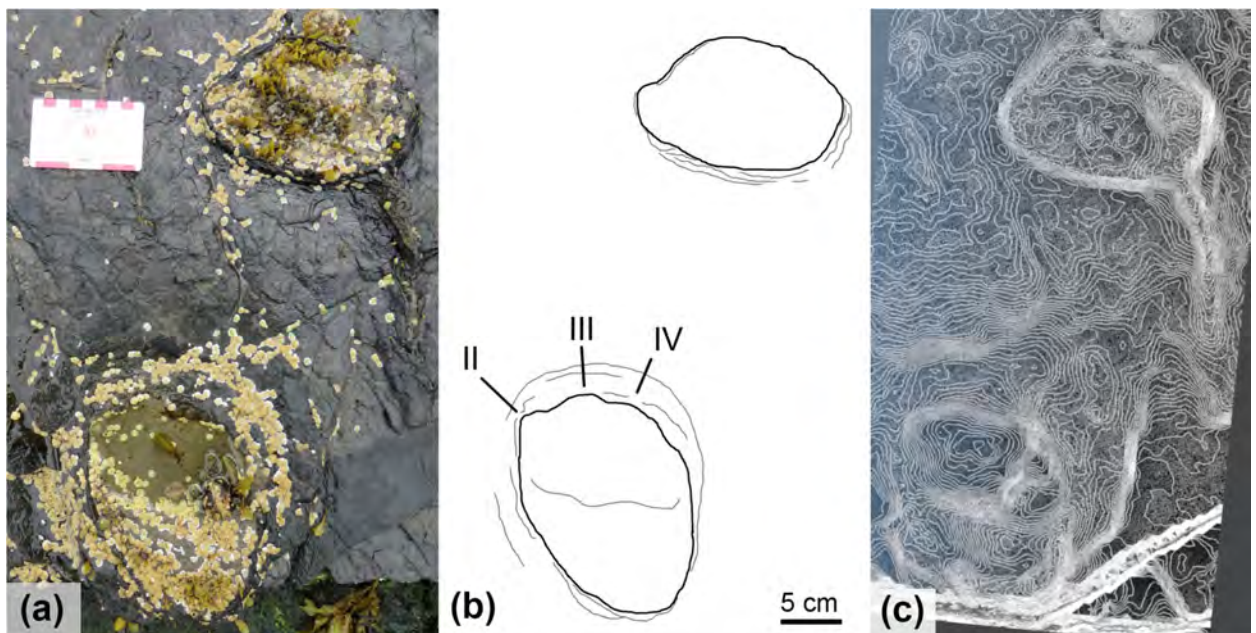


**Fig 7. Exemplar manus/pes pair from BP1\_Twy\_01 at BP1.** (a) Field photograph, (b) outline drawing, and (c) contour map of a right manus/pes pair from BP1\_Twy\_01 highlighting the sediment deformation around each track.

<https://doi.org/10.1371/journal.pone.0229640.g007>

The trackway is 60 cm long (excluding the weakly associated tracks) and oriented at 105°. The manus and pes pace lengths are both ~60 cm. The stride length is ~52 cm between RP1 and RP2. The pes pace angulation is 51.7°. and the width of pace angulation (WAP) of the trackway is ~49 cm.

Several isolated tracks (BP1\_03, BP1\_05, and BP1\_14; Fig 8) on the platform show similar morphologies to those that compose BP1\_Twy\_01. BP1\_03 is an impression with the remnants of an in-filling cast forming a thin drape over its base. BP1\_03 measures 23.8 cm along its long axis and 14.7 cm along its short axis. It has an elongate, subtriangular shape with a rounded, narrow posterior margin widening to the broadest portion of the track near its anterior edge. One of the lateral margins of BP1\_03 is slightly concave while the other is more nearly straight to convex. No clear digits are observed on BP1\_03. BP1\_05 and BP1\_14 are both casts filling impressions and are more sub-oval to sub-circular in shape than BP1\_03. These more rounded shapes could result, in part, from the influence of the infilling material (which can alter the shape of the underlying track). BP1\_05 measures 20.6 cm on its long axis and 16.9 cm on its short axis while BP1\_14 measures 21.2 cm and 18.5 cm, respectively. The track margins of BP1\_05 are smooth and one of the margins parallel to the long axis of the track is slightly convex while the other is slightly concave. Some soft-sediment deformation-related ridging is present immediately adjacent to the convex margin of the track. The margins parallel to BP1\_05's short axis are nearly straight. Although the long axis margins in BP1\_14 exhibit similar curvatures to BP1\_05, BP1\_14 is notable for preserving hints of a left lateral digit. The lateral margins of the track are straight but angled outwards from a narrower heel toward a broader anterior margin. A large mudcrack propagates outward from the right edge of BP1\_14.

The pes impressions of BP1\_Twy\_01 share many features with the ichnotaxon *Deltapodus* [73, 74]. They are generally subtriangular and broaden from a narrower heel to their maximum width near the anterior margin. Additionally, the pes impressions are mesaxonic with three blunt, but subtle digits along the anterior edge. The lateral margins of the pes impressions and the long axis margins of BP1\_03 are nearly straight with minimal curvature as observed in *Deltapodus brodericki* [74]. The manus impressions of BP1\_Twy\_01 are congruent with those of *Deltapodus brodericki* in possessing a convex anterior margin, being shorter than they are wide, and in being entaxonic. The trackway's manus impressions differ from those of *Deltapodus brodericki* in being more rounded (rather than having a more pronounced crescentic shape) and in having smooth edges rather than a more irregular outline. Additionally, the pollex impressions in *Deltapodus brodericki* can constitute up to 1/7 overall width of the manus [74], while the protrusion observed on BP1\_08 (the most distinct manus) is much less pronounced. A final difference between the tracks at BP1 and the Yorkshire *Deltapodus* is their length/width ratios with the BP1 tracks showing lower ratios (1:1.5, manus; 1:0.75, pes) than the ranges reported for the type series (1:1.75–2.5, manus; 1:1.06–12.5, pes; [73]).

In considering other ichnogenera associated with quadrupedal, non-sauropod trackmakers, it becomes clear that the footprints of BP1\_Twy\_01 most closely resemble those of *Deltapodus*. The tracks of BP1\_Twy\_01 are similar to those of *Stegopodus* [75, 76] in possessing a tridactyl pes. However, the pes of *Stegopodus* is transverse (wider than long) with a short heel trace and clearly defined digits with clear hypices between them [75, 76]. In contrast, the pes of *Deltapodus* is longer than it is wide and preserves a more pronounced, elongate heel [73, 74]. Additionally, the manus of *Stegopodus* preserves four distinct digits and is ectaxonic (possessing longer outer digits than inner digits) in contrast with the pronounced pollex impression and consequently entaxonic manus of *Deltapodus*. The footprints of BP1\_Twy\_01 preserve a tridactyl pes that is longer than it is wide and a weakly entaxonic manus and are therefore more consistent with *Deltapodus* than with *Stegopodus*. *Tetrapodosaurus* [77, 78] and *Metatetrapous* [79,

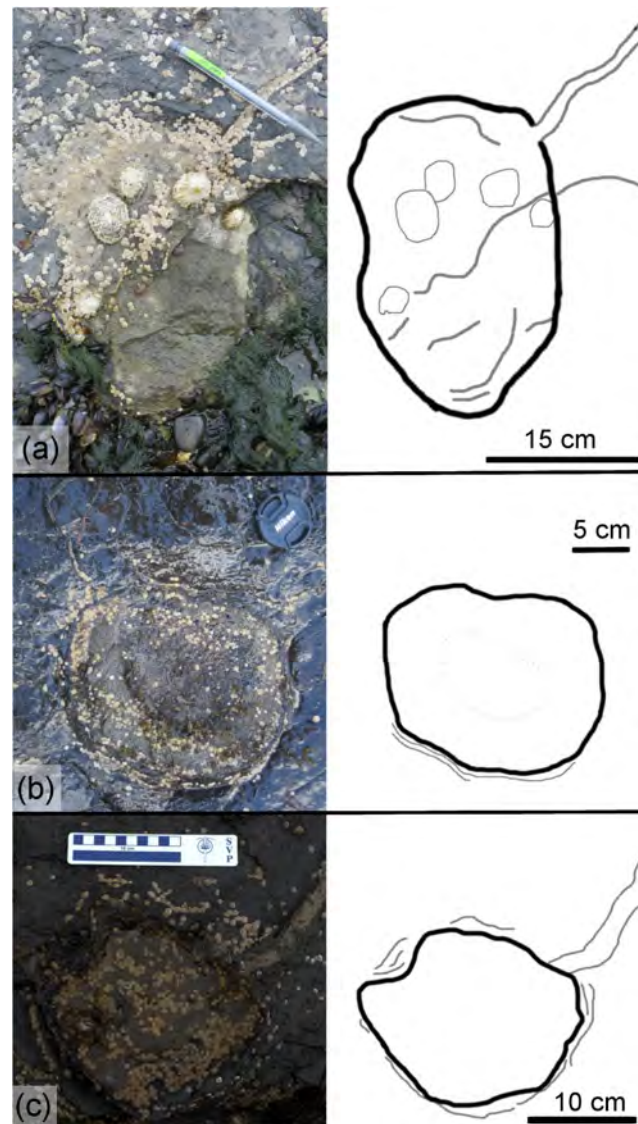


**Fig 8. Isolated tracks with similar morphology to BP1\_Twy\_01 at BP1.** Several isolated tracks at BP1 show similar morphologies to those of quadrupedal trackway BP1\_Twy\_01 from the elongate, subtriangular shape of BP1\_03 (a) to the sub-circular presentations of BP1\_05 (b) and BP1\_14 (c).

<https://doi.org/10.1371/journal.pone.0229640.g008>

80] are characterized by a tetradactyl pes with distinct toes. The unguat impressions of *Tetrapodosaurus* are more blunted than the conical ones preserved in *Metatetrapous*. These ichnogenera contrast with *Deltapodus*' tridactyl pes that lacks pronounced individual digits. In these respects, the footprints of BP1\_Twy\_01 are more consistent with *Deltapodus*.

Therefore, despite slight differences in the presentation of the manus and the narrower track aspect ratios, the sum of the observed features supports the assignment of the tracks in BP1\_Twy\_01 to the ichnogenus *Deltapodus*. Additionally, isolated tracks BP1\_03, BP1\_05, and BP1\_14 also conform to the morphological variations expected of *Deltapodus* tracks (Fig 8). These isolated tracks resemble alternative morphologies in the type series for *Deltapodus* (cf. Fig 3C and 3F, [74]). In particular, BP1\_03 exhibits the elongate subtriangular shape, which

motivated the naming of the ichnogenus [73], while BP1\_05 and BP1\_14 both match the more sub-circular morphologies illustrated.

An important caveat in this discussion is that all of the tracks (including the exemplar tracks BP1\_07 and BP1\_08) are at least partially infilled by sediment. Sediment infills can distort tracks in a variety of ways including (1) changing linear measurements like track length, (2) smoothing track margins, and (3) potentially filling other abiotic features (which would give the track an anomalous shape).

1. While linear measurements can be affected by sediment infilling, the majority of the comparisons that underlie this ichnotaxonomic work rely upon the interactions of multiple measurements (i.e. investigating the aspect ratio of the track). We reason that, unless there is an external factor like a plane of weakness in the surrounding rock, sediment infills would distort the different track axes to a similar extent. Thus, it seems unlikely that the overall aspect ratio of tracks would radically change (i.e. that a track which has an antero-posteriorly directed long axis would not, under the influence of infilling sediment, develop a mediolaterally directed long axis). This reasoning is important when aspect ratio is one of the key factors that differentiates the *Deltapodus* pes (which is anteroposteriorly elongated) from the *Stegopodus* pes (which is mediolaterally elongated). We reason that, despite the sediment infills, the elongate nature of the pes of BP1\_07, supports reference to *Deltapodus* over *Stegopodus*.
2. Sediment infills can result in the smoothing of track margins. Functionally, that implies that protruding features (like digits) have the potential to become less pronounced. This effect is indeed a concern as both the three pes digits and the pollex impression of BP1\_07 and BP1\_08, respectively, are weakly indicated in the track margin. However, on similar reasoning to the above concern about linear measurements, one would expect the smoothing to occur in a way commensurate with the original extent of features. Since the digits of both *Tetrapodosaurus* and *Metatetrapous* are roughly symmetric across the center of the foot, it could be expected that they would be reduced in similar fashions. Thus, in this context, it does not seem likely that the sediment infilling the tracks of BP1\_Twy\_01 could result in initially tetradactyl tracks appearing tridactyl. Additionally, the presence of a weakly defined pollex on BP1\_08 without indication of any other digits in the anterior margin of the track hints that, prior to sediment infilling, this digit was more pronounced. This inferred pronounced pollex is again consistent with the morphology expected for *Deltapodus*.
3. Finally, we can investigate the potential for infilling of abiotic features causing anomalous shapes within these tracks by examining how these infills interact with extensive mudcracks on the trackbearing surface. A mudcrack propagates from the posterior margin of BP1\_08 (the manus impression of the exemplar pair of tracks associated with BP1\_Twy\_01; Fig 7). However, the raised lip of the displacement rim clearly defines the track margins and no clear distortion along the plane of weakness introduced by the mudcrack is observed. Thus, in context of this particular trackway, it appears that the infilling sediment was not emplaced in such a way that existing, clearly abiotic features that intersected with the track introduced anomalies into the perceived shape of the track.

For these reasons, we feel confident that, although the shape of these footprints has undoubtedly been affected by subsequent, post-registration taphonomic process (like infilling), it remains most consistent with the ichnogenus *Deltapodus*.

Despite the similarity in shape and characteristics between the tracks at BP1 and the type *Deltapodus* tracks from Yorkshire, there are several apparent differences between the two assemblages—particularly in track size and trackway gauge.

The majority of the *Deltapodus brodricki* tracks from Yorkshire have lengths of >25 cm (avg. length of ~35 cm with a standard deviation of ~8.8 cm) and *Deltapodus* tracks of a similar size are reported in the western US, Spain, and China [73, 74, 81–84]. The size of the Skye *Deltapodus* tracks (avg. length of 18.25 cm with a standard deviation of 3.59 cm), therefore, seems quite small (approximately half the size of other observed tracks). However, rare tracks from Yorkshire and an additional report of *Deltapodus* from Morocco (length 16.6 cm) extend the size range for the ichnogenus to encompass that of the Skye tracks (Fig 9) [85, 86]. Thus, the Skye tracks fall within the size range observed for *Deltapodus* globally, albeit at the lower end of the range, and may indicate that the trackmaking individuals were indeed smaller bodied than the Yorkshire trackmakers (i.e. either juveniles or members of a smaller-bodied species).

The quadrupedal trackway at BP1 exhibits a wide gauge for *Deltapodus*-like trackways, with tracks made by the left manus and pes and tracks made by the right manus and pes separated by ~49 cm. This contrast can be appreciated qualitatively by comparing BP1\_Twy\_1 (Fig 10A) with the type *Deltapodus* trackway from Yorkshire (Fig 10B). The observation of a wider gauge holds even when normalized for track size using the trackway ratio (*sensu* [52]). The average pes trackway ratio for the type tracks is 29.5% while the average trackway ratio for the Skye trackway is ~23.5% (in the case of this metric, the ratio decreases as the gauge increases). It has been suggested that quadrupedal trackway gauge relates at least in part to both the gait of the organism and the nature of the substrate over which it travels [51, 87, 88] (*contra* [89]) and some of these behavioral or environmental factors may be at play in the case of the wide gauge of this particular trackway.

The hip heights of the BP1 *Deltapodus* trackmaker estimated using Eqs 3 and 4 were quite similar (~68 cm and ~72 cm, respectively) and indicate that this trackmaker stood ~70 cm at the hip. The progression (distance which the individual travels with a step) of the trackway is low (~5.9 cm) as a result of the extremely wide gauge of the trackway. The speed at which the individual was traveling is estimated to be a walking pace of 40 cm/s (1.45 km/hr). Thus, the trackmaking individual, in this case, was both quite small and moving quite slowly.

**Bipedal trackways.** In addition to the quadrupedal trackway, BP1\_Twy\_01, a set of associated tracks and two bipedal trackways are present at the site. The track association (TA\_1) consists of three clear tracks with diagnostic features. BP1\_Twy\_02 and BP1\_Twy\_03 each consist of more ambiguous tracks.

TA\_1 (Fig 11 and S1 Appendix) is located on the southwestern corner of the tracksite and is separated from the main track-bearing platform by a narrow strip of sand. BP1\_30 and BP1\_32 both appear to be right pes impressions that are infilled with limestone casts. BP1\_31 is an impression that does not have an infilling sediment. It shows less distinctive track boundaries and is primarily recognizable through localized sediment deformation and bowing in the underlying shale layers near its posterior margin. The preservation grade [39, 40] of tracks that compose TA\_1 ranges from 0 (BP1\_31) to 1 (BP1\_30, BP1\_32).

The tracks composing TA\_1 are tridactyl and mesaxonic with narrow, sharply pointed digits (Fig 12). The average length (L) of the tracks is ~39 cm. The heel is narrow, elongated, and tapers to subtriangular posterior margin. The track interdigital angles exhibit a relatively broad range from 20.5° to 35°. Although both BP1\_30 and BP1\_32 are broken and lack a lateral digit, the remaining lateral digits have a sigmoid curve (likely from the motion of the foot through the substrate). Both BP1\_30 and BP1\_32 hint at an overall asymmetry in track shape (with BP1\_30 showing a straight lateral margin below digit IV and BP1\_32 showing a slight

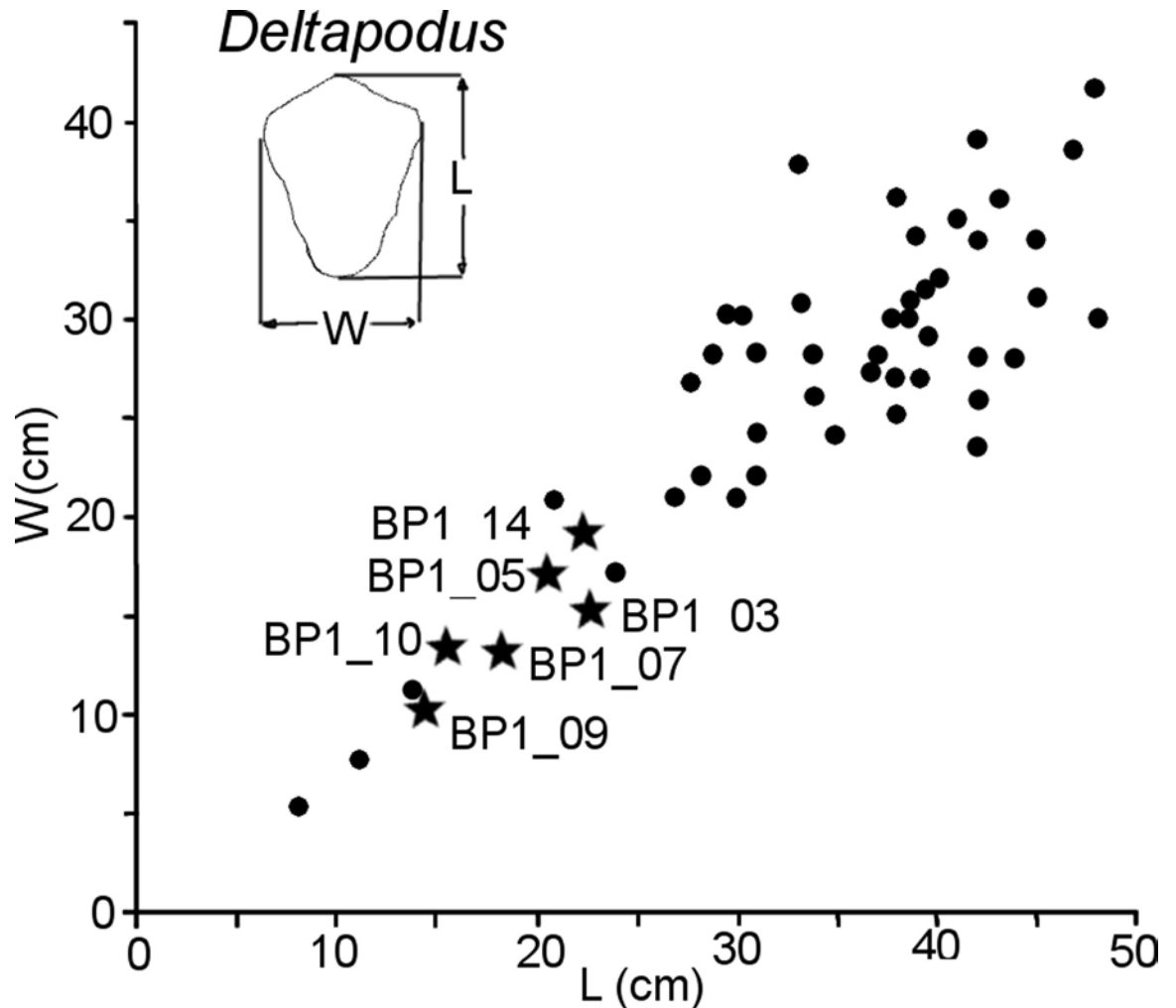


**Fig 9. Relative sizes of Skye and Yorkshire *Deltapodus* tracks.** The Skye quadrupedal tracks (shown as stars) are plotted with known *Deltapodus* track measurements from Yorkshire (redrafted and modified from Fig 13, [85]). All Skye tracks fall within the general size trends for the ichnogenus.

<https://doi.org/10.1371/journal.pone.0229640.g009>

notch in the lateral margin below digit II). It is not possible to evaluate whether phalangeal pad impressions are present in these tracks due to the presence of infilling sediment.

Since BP1\_30, BP1\_31, and BP1\_32 are located very near one another on the platform, are all about the same size, and all face in generally the same direction, it is tempting to group them as all being made by the same individual. However, grouping all three tracks into a single trackway requires a non-parsimonious interpretation of the animal's locomotion (a lateral step within an already wide gauge stance). Therefore, it is unlikely that all three tracks constitute a trackway. However, it is also unlikely that all three footprints are completely unrelated to one another, particularly because they all are facing approximately the same direction on a track-bearing platform that does not show a dominant direction with regard to track orientation. It is more likely that two of the tracks are associated with a single individual and that the third track is from a different instance of an individual walking across the platform. When considering which tracks look most similar, the grouping of BP1\_30 and BP1\_32 into a partial trackway seems to be favored as both show similar limestone infillings, levels of preservation, and track characters (including a sigmoidal shape in the lateral digits). However, associating these

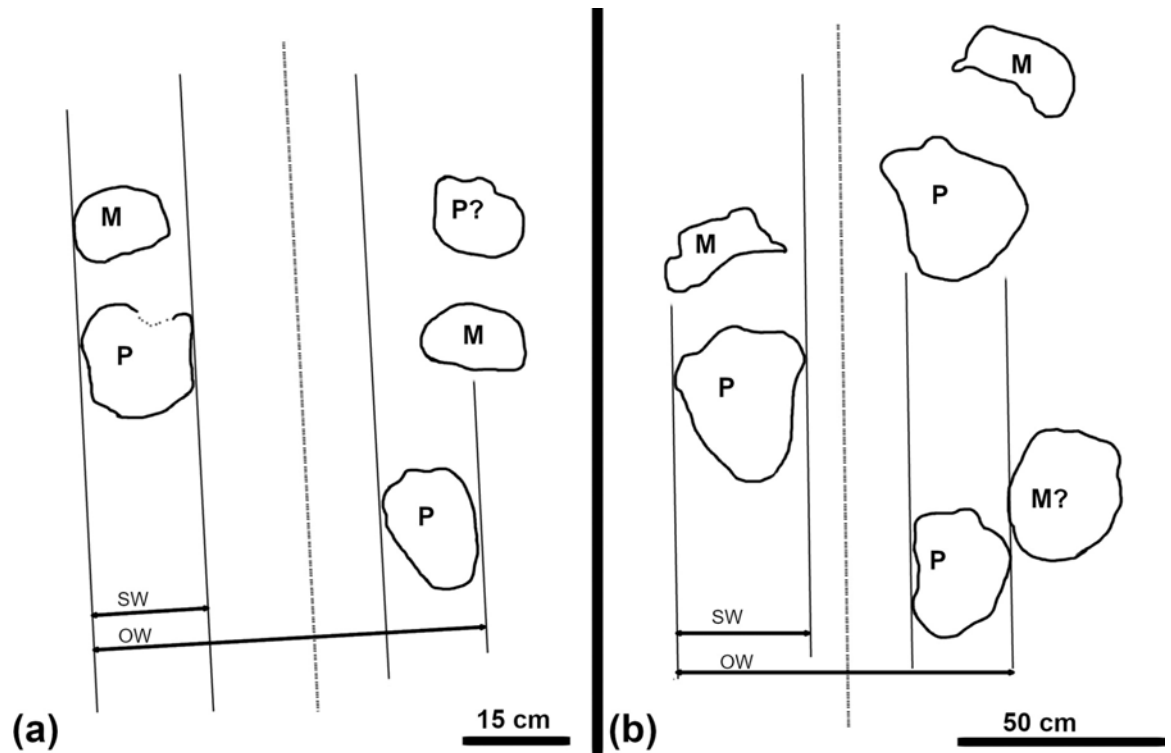


**Fig 10. Comparison of *Deltapodus* trackway gauges.** (a) The Skye trackway shows a wider gauge than (b) the type *Deltapodus* trackway (redrafted from Fig 7, [63]). M denotes manus impressions, P denotes pes impressions, SW denotes the side width, and OW denotes the outer width. The trackway midline is denoted by a gray dashed line.

<https://doi.org/10.1371/journal.pone.0229640.g010>

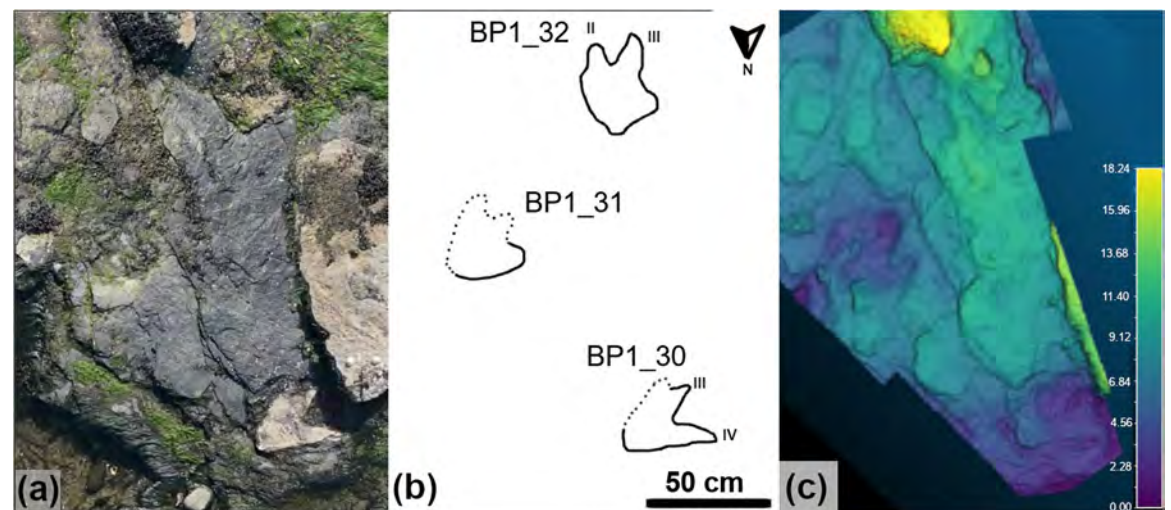


**Fig 11. Overview of TA\_1.** TA\_1 shown from (a) the model orthophoto, (b) as a line drawing, and (c) as a false color depth rendering. The three tracks composing the trackway present a variety of preservation styles, with BP1\_30 and BP1\_32 preserved as limestone casts and BP1\_31 as a shallow impression. The impression can be seen in the orthophoto by looking both at subtle changes in vegetation and shading along the left margin and can be more clearly visualized using the false color depth rendering. The color scale of (c) is in units of cm.

<https://doi.org/10.1371/journal.pone.0229640.g011>

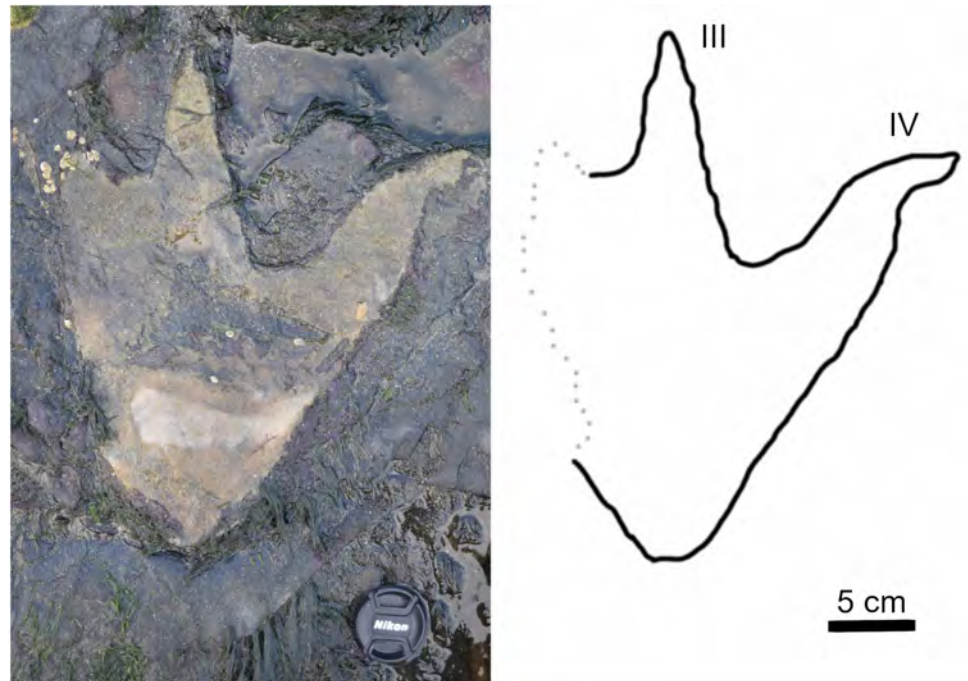


**Fig 12. Exemplar track BP1\_30.** A field photograph and corresponding outline drawing showing the distinctive limestone cast infilling the impression of BP1\_30, the most clearly defined track in TA\_1. The strong color contrast between the rock types serves to accentuate the shape details of the track including the narrow, pointed digits and the elongated heel.

<https://doi.org/10.1371/journal.pone.0229640.g012>

footprints together in the same partial trackway would necessitate a bipedal individual with a relatively wide stance and fairly extreme rotation of the feet away from the track midline. Additionally, both tracks appear to be right pes impressions which raises the question of where the missing left pes impression between them is. In light of this, the group of BP1\_31 and BP1\_32 seems to be the most likely scenario with the resultant trackway exhibiting a very narrow gauge and strong inward rotation of both feet. Although BP1\_31 and BP1\_32 are favored as a grouping with BP1\_30 being the track formed by an unrelated individual walking in a similar direction, we refer to all three tracks as a track association (TA\_1) to reflect continued uncertainty about how these tracks can best be associated with one another.

For BP1\_30 and BP1\_32 (the two better-preserved tracks in TA\_1), their general morphology (elongate track shape and narrow toes) suggests a likely theropod affinity for the trackmaker. However, the measured track parameters (Table 1), show a mixture of theropod and ornithopod affinities. Both assessed tracks displayed a slightly greater ornithopod affinity based on whole track characteristics, while parameters specifically focused on ratios from digit measurements tended to yield strong theropod affinities. Due to the overall shape of the tracks (particularly the pointed nature of the toes), the 'digit-focused' parameters are considered more representative of trackmaker, which we interpret to most likely be a theropod.

Since these tracks have low preservation grades and outlines that are heavily influenced by the in-filling sediments, they cannot be confidently assigned to any ichnogenus. Although a firm ichnotaxonomic diagnosis cannot be made, we observe that these tracks share some similarities with the ichnogenus *Megalosauripus* [90] and could be further discussed with reference to this ichnogenus. The tracks conform to the diagnostic characteristics of this ichnogenus in being large, tridactyl, and having an elongate heel relative to digit III [90]. [50] observes that

**Table 1. Track parameters and assessment of the trackmaker affinity of TA\_1 at BP1.**

Track Parameters	Threshold values and probability that the track is either theropod or ornithopod	BP1_30	BP1_32
L/W	80.0% Theropod > 1.25 > Ornithopod 88.2%	n/a	n/a
L/K	70.5% Theropod > 2.00 > Ornithopod 88.0%	1.37	1.79
L/M	65.0% Theropod > 2.00 > Ornithopod 90.7%	1.77	1.93
BL2/WMII	76.1% Theropod > 2.00 > Ornithopod 97.4%	n/a	2.35
BL3/WMIII	72.7% Theropod > 2.20 > Ornithopod 97.7%	4.34	2.27
BL4/WMIV	76.1% Theropod > 2.00 > Ornithopod 97.6%	2.95	n/a
LII/WBII	84.6% Theropod > 3.75 > Ornithopod 90.2%	n/a	4.12
LIII/WBIII	70.6% Theropod > 4.00 > Ornithopod 91.5%	4.37	4.40
LIV/WBIV	73.7% Theropod > 3.75 > Ornithopod 93.4%	4.55	n/a

Track measurements (as outlined in Fig 2) from TA\_1 were used to determine the likelihood of the track having either theropod or ornithopod affinity [42]. Both tracks demonstrated a slightly more ornithopod affinity based on whole track characteristics, while more 'digit-focused' parameters consistently yielded a theropod affinity. The blank spaces in the table reflect parameters that are incalculable because the track was broken.

<https://doi.org/10.1371/journal.pone.0229640.t001>

some *Megalosauripus* tracks have pointed claw marks and have low (22–40°) interdigital angles. TA\_1 manifests all of these characteristics, with the tracks only differing from the extended description of [50] in lacking a “squared U-shaped metatarso-phalangeal impression”.

Interestingly, *Megalosauripus* tracks exhibit some of the supposed 'ornithopod' affinities seen in the Skye tracks, particularly a low length to width ratio. *Megalosauripus* tracks, while still being elongate, tend to have a lower length to width (L/W) ratio than other large theropod ichnogenera. For example, the L/W ratios of BP1\_30 and BP1\_32 (1.20 and 1.14) fall near to the range of ratios (1.24–1.39) described for ~80 *Megalosauripus* tracks from Portugal [50]. This ratio is far below the observed L/W ratios for the large theropod ichnogenus *Eubrontes* (~1.5, measured and averaged from Fig 5A and 5B [91]). The tracks of TA\_1 do not correspond with *Eubrontes* because they lack distinctive phalangeal pad impressions and digit III has a shorter relative length and parallel (instead of spindle-shaped) sides [90, 91]. *Kayentapus* [92, 93] is another large theropod ichnogenus with a low L/W ratio caused by relatively broad interdigital angles ((II^III) = ~34 and (III^IV) = ~29). These values were averaged from UCMP 83668–1 and UCMP 83668–4, the two most distinct tracks of the type trackway [93]. However, TA\_1 has a lower L/W ratio than *Kayentapus* and smaller interdigital angles. Additionally, the constituent tracks of TA\_1 do not show the pronounced extension of digit III evident in the type series of *Kayentapus*. Furthermore, although it should be noted that this features are strongly controlled by the nature of the substrate, TA\_1 does not correspond to *Kayentapus* because the extent of their 'heel' is more pronounced than the strongly digitigrade presentation observed in the type series [92, 93]. The presence of the distinctive phalangeal pad impressions associated with *Kayentapus* could not be assessed for these tracks because the infilling sediment obscures the base of the track.

The two bipedal trackways, BP1\_Twy\_02 and BP1\_Twy\_03, are not as well-preserved as TA\_1. BP1\_Twy\_02 (Fig 13; link in S1 Appendix) is located towards the center of the main track-bearing platform. Its line of progress is generally southward and the trackway seems to emerge from underneath the overlying limestone bed. The trackway consists of three tracks (BP1\_16, BP1\_17, and BP1\_18). The first two are positive relief casts while the third track is a shallow impression. The casts are crosscut by large desiccation cracks. The preservation grade [39, 40] of the positive relief casts is 1 while the shallow impression does not preserve clear morphological details and is therefore at grade 0. BP1\_Twy\_03 is located on the southern side

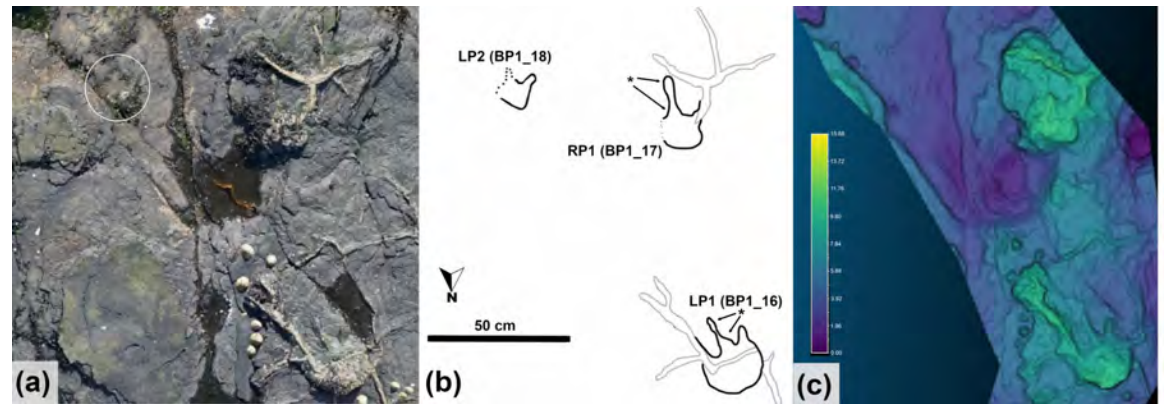


**Fig 13. Overview of BP1\_Twy\_02.** (a) The orthophoto of BP1\_Twy\_02 is shown with (b) a line drawing highlighting distinctive features of both the tracks and the desiccation cracks that preferentially propagate from the toes of the tracks and (c) a false color depth map of the trackway. The line drawing particularly emphasizes the presence of phalangeal pads on digit III of LP1 and RP1 with arrows (labeled \*) pointing out their location within the tracks. The white circle on the (a) shows the location of BP1\_18 since it is difficult to discern in both the orthophoto and the depth map. The color scale of (c) is in units of cm.

<https://doi.org/10.1371/journal.pone.0229640.g013>

of the track-bearing platform. BP1\_Twy\_03 (Fig 14, link in S1 Appendix) is the most poorly preserved of the trackways at the site. The preservation grade [39, 40] of the tracks in BP1\_Twy\_03 is 1 for exemplar track BP1\_26 and 0 for the subsequent deep impressions.

BP1\_Twy\_02 is 1.73 m long with an orientation of  $155^\circ$ . The average pace length is  $\sim 79$  cm and the stride length is 1.45 m. The pace angulation is  $131^\circ$  and the width of pace angulation (WAP) of the trackway is 50 cm. The individual track rotation for BP1\_Twy\_02 is towards the midline (negative angle). BP1\_Twy\_03 is oriented at  $\sim 100^\circ$  and is 3.8 m long. The pace and stride lengths are essentially regular throughout the trackway. The average pace length is 1.19 m and the average stride length is 2.31 m. The average pace angulation of the trackway is  $153^\circ$ .

Although many of the features of the positive relief casts in BP1\_Twy\_02 were later obliterated by the propagation of the desiccation cracks, BP1\_16 and BP1\_17 show widenings of digit III that could be the remnants of phalangeal pads (Fig 15A). Two such widenings are on each track: one at the base of digit III and the other at the most distal end of the digit. In addition to the long, narrow toes exhibited by each track in the trackway, the presence of these pads strengthens the inference that the trackmaker was a theropod. The presence of distinctive phalangeal pads along the toes is more characteristic of theropod tracks than ornithomorph tracks [94]. Although the presence of probable phalangeal pads on the tracks suggests that the component tracks of BP1\_Twy\_02 are more likely made by a theropod trackmaker, we refrain from assigning them to a ichnogenus.

The only track in BP1\_Twy\_03 that displays distinctive features is BP1\_26—the first track in the trackway sequence. Like the majority of the other tracks at the site, BP1\_26 (Fig 15B) is a modified true track since it is infilled by a limestone cast. Both edges of the track are broken and only one digit (III) is clearly visible. It is likely that the track was originally tridactyl and mesaxononic. The length of the BP1\_26 is  $\sim 33$  cm, which places the bipedal trackmaker in the large size category. This track length was used for subsequent hip height and speed estimations (Table 2) as the features of the other tracks composing the trackway were indistinct. The other tracks in BP1\_Twy\_03 (BP1\_27, BP1\_28, and BP1\_29) are deeply impressed in the underlying shale bed, display indistinct margins, and are partially infilled with limestone casts. Although the track impressions are deep (as seen in particularly with BP1\_27 in Fig 14C), the angles of the bedding deflections around them are shallow. The highly localized sediment deformation

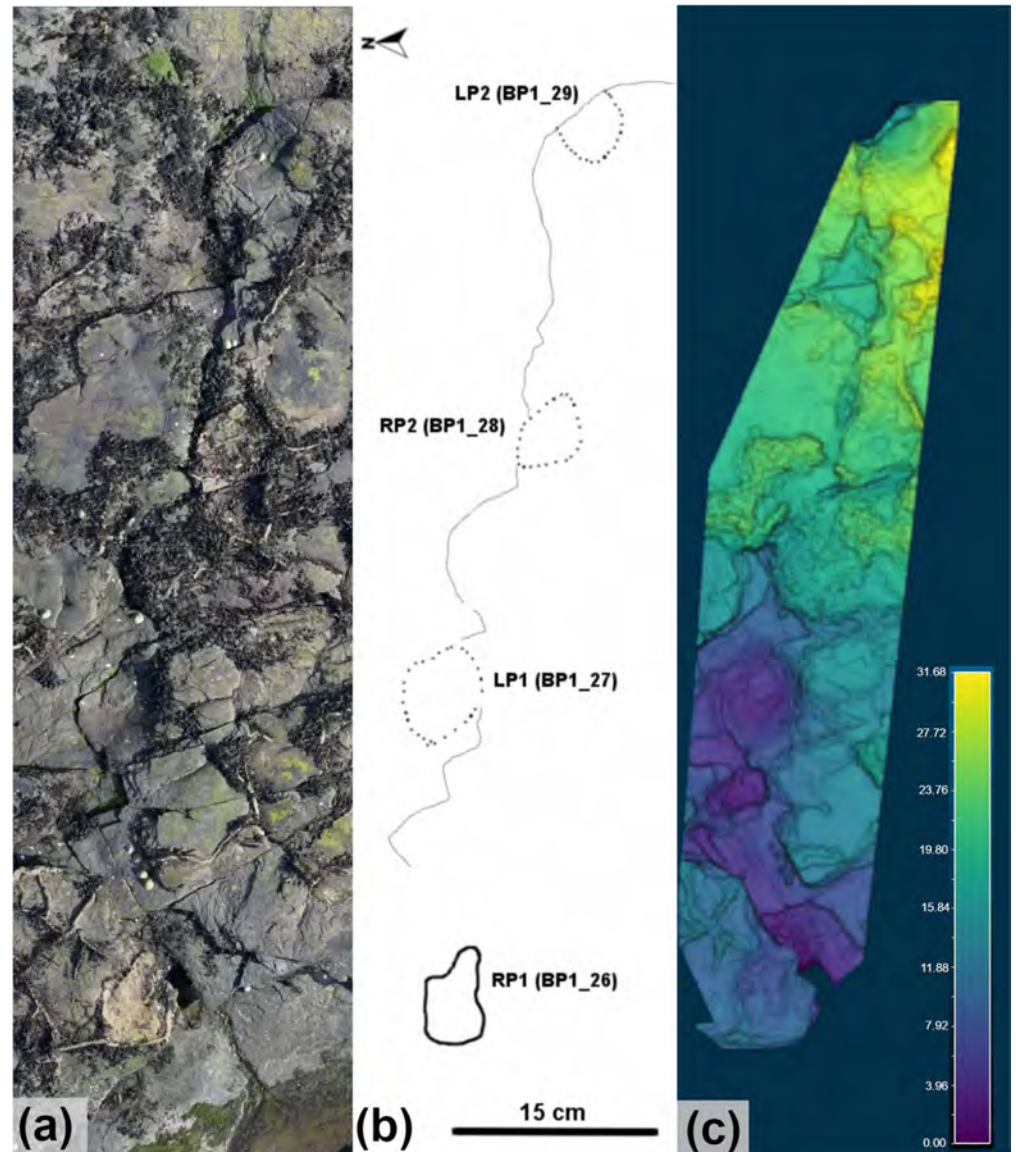


**Fig 14. Overview of BP1\_Twy\_03.** BP1\_Twy\_03 is shown as an (a) orthophoto, (b) a line drawing, and (c) a false color depth map. The trackway spans the whole southern portion of the main track-bearing platform with BP1\_29 being present solely as a broken heel mark on the platform edge. The color scale of (c) is in units of cm.

<https://doi.org/10.1371/journal.pone.0229640.g014>

around the tracks, which is particularly visible along the platform edge with BP1\_29 (LP2), indicates that these impressions are indeed footprints.

All measurements related to the bipedal trackways at BP1 are summarized in [Table 2](#).

Since variations in the shape of dinosaur footprints result from the combination of gross pedal morphology, the motion of the foot through the substrate, the consistency of the substrate, and post-registrational taphonomic processes [40, 59], variations in track morphology observed in the trackways and track association the site do not definitively imply that there are multiple trackmaking theropod species at BP1. Using an average of the track lengths in each trackway, the hip heights of the trackmakers for BP1\_Twy\_02, BP1\_Twy\_03, and TA\_1 were calculated ([Table 3](#)). Relative stride lengths ( $S/h$ ) of  $<2$  indicate walking gaits for the two trackway trackmakers ([Table 3](#)).

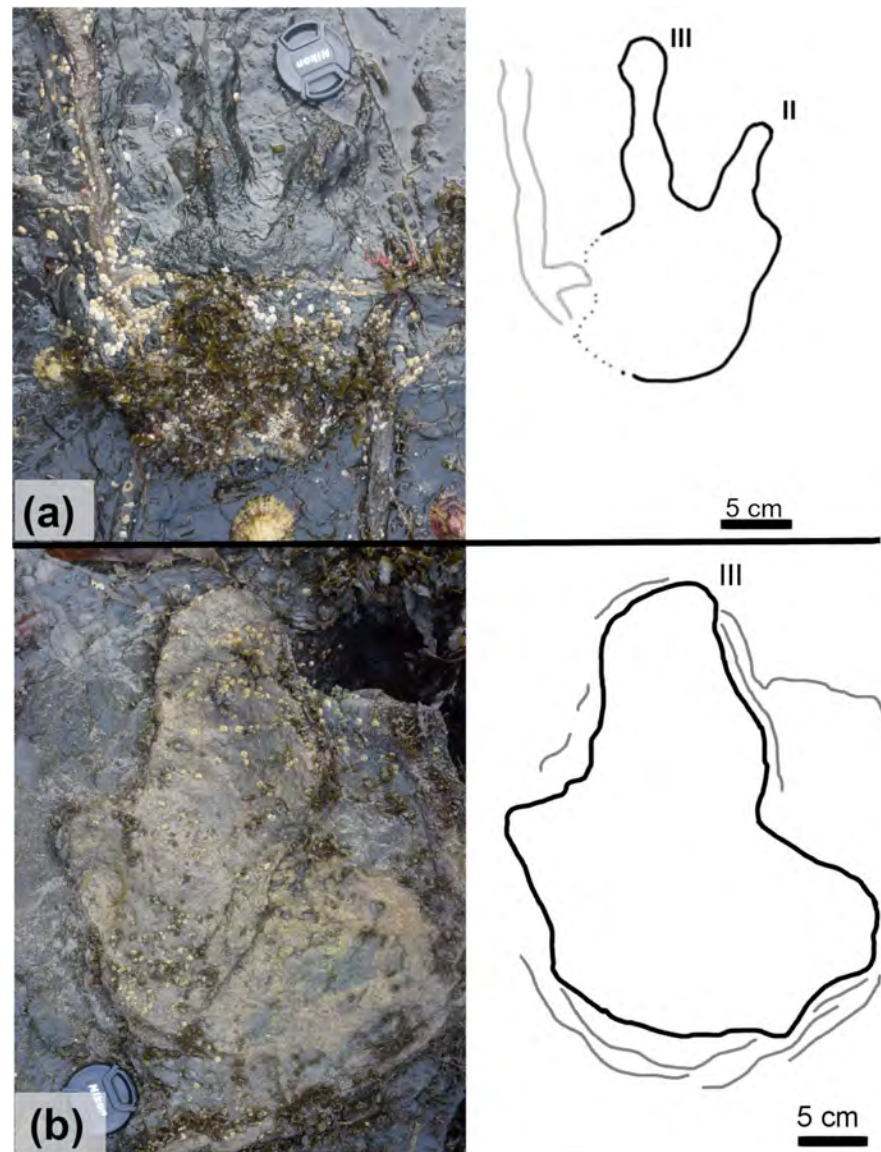


**Fig 15. Exemplar tracks from BP1\_Twy\_02 and BP1\_Twy\_03.** (a) A field photograph and outline drawing of BP1\_16 illustrating the presence of remnant phalangeal pads on the positive relief casts present in BP1\_Twy\_02. (b) A field photograph and outline drawing of the most clearly defined tracks in BP1\_Twy\_03 (BP1\_26). The track is preserved as a broken limestone cast (modifying the true track) set in an area of strong sediment deformation. This deformation is illustrated on the line drawing as thin gray lines concentrated around the track's heel.

<https://doi.org/10.1371/journal.pone.0229640.g015>

While [53]'s formulation to estimate hip height is a coarse measurement (due to variation of the anatomy/posture of different organisms and the effects of substrate and dynamic motion on the pes length), the wide range in estimated sizes for the theropod tracks at the site (~116 cm to ~155 cm) hints that at least two individuals traversed the mudflat.

**Additional tridactyl track morphologies.** BP1\_01 (Fig 16A) is located in the northwestern-most portion of the track-bearing platform. The track is eroded and is missing one of the lateral digits. Since the track is not associated in a trackway, digit numbering is arbitrary with the complete left lateral digit referred to as digit I and the incomplete right lateral digit as digit IV. BP1\_01 is mesaxonic and tridactyl. The digits taper to slightly pointed tips (but do not

**Table 2. BP1 bipedal trackway measurements.**

	N	RP[1]	RP[2]	LP	S[1]	S[2]	WAP[1]	WAP[2]	$\gamma$ [1]	$\gamma$ [2]	$\alpha$	Length	Orientation
BP1_Twy_02	3	0.70	n/a	0.88	1.45	n/a	0.50	n/a	131	n/a	-10.4	1.73	155
BP1_Twy_03	4	1.28	1.04	1.24	2.34	2.28	0.39	0.50	150	156	n/a	3.80	100

The measurements of the bipedal trackways present at Brother's Point Site 1 are summarized here. All measurements are in meters except for  $\gamma$ ,  $\alpha$ , and trackway orientation (measured in degrees). N is the number of tracks in each trackway. RP[1] and RP[2] are the right pace measurements taken between RP<sub>x</sub> and LP<sub>x</sub> of the trackways respectively (track designations figured on outline drawings). LP represents the left pace measurements. S[1] and S[2] are the stride lengths between the right feet and the left feet, respectively, in BP1\_Twy\_03 and S[1] denotes the only measurable stride length in BP1\_Twy\_02. For BP1\_Twy\_03, WAP[1] is the trackway width measured between RP1 and RP2 with LP1 as the focal point while WAP[2] is the trackway width measured between LP1 and LP2 with RP2 as the focal point. WAP[1] for BP1\_Twy\_02 denotes the trackway width measured between stride line and the opposite footprint (RP1).  $\gamma$  is the pace angulation of the trackway. For BP1\_Twy\_03,  $\gamma$  is the pace angulation with [1] using RP1 as the vertex of the angle and [2] using LP2 as the vertex of the angle.  $\alpha$  measures the track rotation of footprints with regard to the midline. LP1 in BP1\_Twy\_2 demonstrates inward rotation (a negative angle).

<https://doi.org/10.1371/journal.pone.0229640.t002>

show distinctive claw impressions) while the heel of the track is moderately broad. The preservation grade [39, 40] of this track is 1.

The track length is 32.5 cm, which places it in the large bipedal size class (S1 Appendix of S2 Table). The interdigital angle between digit II and digit III is 30.7°. The affinity of this track is difficult to assess qualitatively because elongate toes with pointed tips are associated with theropods while a broad heel is more characteristic of ornithopods. Although not all parameters could be calculated, the likelihood analysis of [42] was used to determine the most likely affinity of BP1\_01 (Table 4).

This probabilistic analysis slightly favored an ornithopod trackmaker but did not result in a strong affinity with either dinosaur clade (Table 4).

The final tridactyl track morphology at BP1 is track BP1\_06 (Fig 16B). BP1\_06 is mesaxonic, tridactyl track with a potentially broad heel and moderately wide toes. Its lateral digits have acted as propagating channels for desiccation cracks. Digit III tapers to a point and preserves the remnants of a probable claw impression. As a result of this impression, BP1\_06 can be framed as one of the most well-preserved of the tracks at this site and, although still ranked as 1, teeters on the edge of preservation grade 2 (where tracks preserve clear toe and ungual marks) [39, 40]. The track is 16.4 cm long and 13.7 cm wide. The interdigital angle between the left lateral digit and digit III is 32° and between the right lateral digit and digit III is 29°.

BP1\_06 is distinctive from the larger tridactyl tracks observed in TA\_1 because of its overall size, the more curved lateral margins of its digits, and because the heel is less elongate (broken). It differs from the tracks of BP1\_Twy\_02 because the digits are broader and from the isolated track BP1\_01 because the digits taper sharply and end in distinctive claw impressions instead of slightly pointed tips. Although the track cannot be assigned to a specific ichnotype

**Table 3. BP1 theropod size and velocity estimations.**

	Approximate Trackmaker Hip Height (cm)	Estimated Velocity	
		m/s	km/hr
BP1_Twy_02	116	1.2	4.4
BP1_Twy_03	131	2.3	8.3
TA_1	155	-	-

Based on the range of hip heights estimated, at least two sizes of bipedal trackmaker were present at BP1 with TA\_1 being made by the largest individual and the trackmaker of BP1\_Twy\_02 estimated to be moving slower than that of BP1\_Twy\_03.

<https://doi.org/10.1371/journal.pone.0229640.t003>

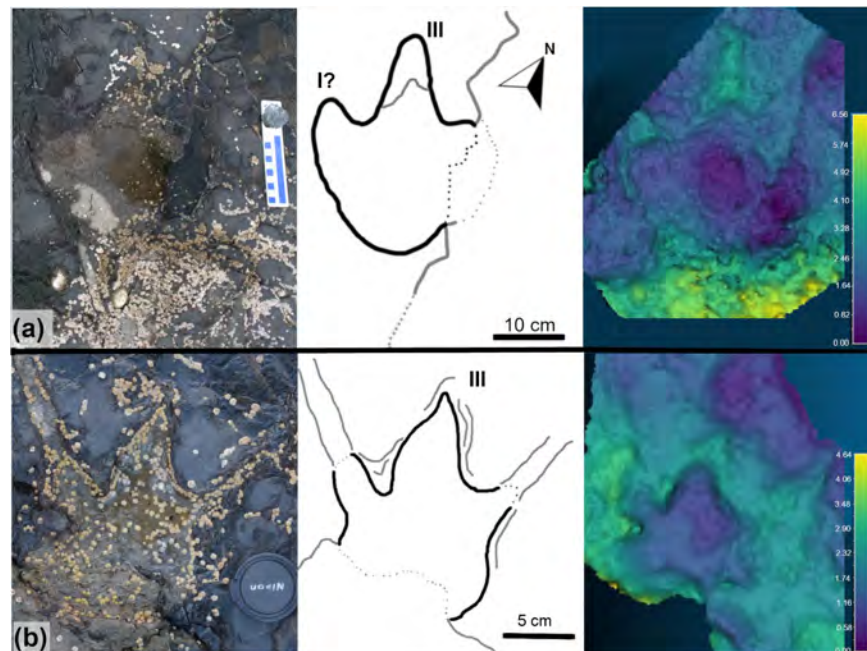


**Fig 16. Additional tridactyl track morphologies from BP1.** (a) Although broken, BP1\_01 (shown with a field photograph, corresponding line drawing, and false color depth map) demonstrates the strongest ornithopod affinity of any of the tracks present at the site. (b) BP1\_06 is shown with a field photo, a corresponding line drawing, and a false color depth map. The track preserves strong sediment deformation around the toes and the hypices and desiccation cracks propagate from the lateral digits. These sedimentary features are denoted with light gray outlines on the line drawing. The diameter of the camera lens is 5 cm. The color scale of both false color depth maps is in units of cm.

<https://doi.org/10.1371/journal.pone.0229640.g016>

because diagnostic characters are lost to the desiccation cracks propagating from both lateral digits and obstruction of the heel by the overlying bed, its presence at BP1 hints at an additional, bipedal trackmaker.

Several other possibly modified tracks are observed at BP1 and represent eroded, in-filled casts with pronounced soft-sediment deformation around them (Fig 17). These non-

**Table 4. Assessment of the trackmaker affinity of BP1\_01.**

Track Parameters	Threshold values and probability that the track is either theropod or ornithopod	BP1_01
L/W	80.0% Theropod > 1.25 > Ornithopod 88.2%	1.32
L/K	70.5% Theropod > 2.00 > Ornithopod 88.0%	1.64
L/M	65.0% Theropod > 2.00 > Ornithopod 90.7%	1.67
BL2/WMII	76.1% Theropod > 2.00 > Ornithopod 97.4%	1.70
BL3/WMIII	72.7% Theropod > 2.20 > Ornithopod 97.7%	4.1
BL4/WMIV	76.1% Theropod > 2.00 > Ornithopod 97.6%	n/a
LII/WBII	84.6% Theropod > 3.75 > Ornithopod 90.2%	3.51
LIII/WBIII	70.6% Theropod > 4.00 > Ornithopod 91.5%	4.27
LIV/WBIV	73.7% Theropod > 3.75 > Ornithopod 93.4%	n/a

Track measurements from BP1\_01 were used to determine the likelihood of the track having either theropod or ornithopod affinity. Comparing the track parameters with [42] results in a further indeterminate result. In terms of overall track shape parameters, the track consistently presents as ornithopod while ratios of the measurements taken on individual digits yield mixed theropod and ornithopod results. The blank spaces in the table reflect parameters that incalculable because the track was broken.

<https://doi.org/10.1371/journal.pone.0229640.t004>

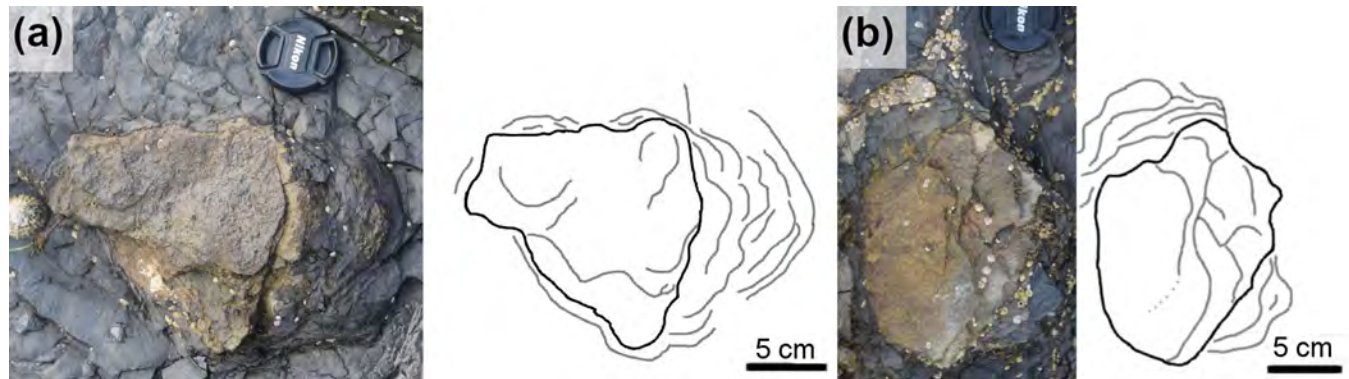


**Fig 17. Eroded and in-filled casts observed at BP1.** Examples of this track type can be seen with (a) BP1\_21 and (b) BP1\_22. These eroded casts are particularly abundant around the margins of the track-bearing platform. The track outlines are shown in black while soft-sediment deformation is illustrated in gray.

<https://doi.org/10.1371/journal.pone.0229640.g017>

diagnostic, broken casts are useful in giving a sense of the relatively high density of tracks on the paleosurface.

### Brothers' point 3

A variety of track morphologies are preserved at Brothers' Point 3. A total of 18 tracks are observed at the site and numbered using a system of BP3\_01, BP3\_02, etc. Overall, two trackways (BP3\_Twy\_01 and BP3\_Twy\_02) are observable. A link to the subsampled photogrammetric model of the concentration of large tridactyl tracks at the outcrop can be found in [S1 Appendix](#).

**Large tridactyl tracks.** BP3\_08 ([Fig 18](#)) is the best preserved and most diagnostic track at the site. It is located along the southern edge of the platform immediately adjacent to BP3\_Twy\_01. The track forms a deep impression in the shale unit with a pronounced deformation rim around the entirety of the track margin. The digit outlines are particularly affected by the sediment deformation, as the shale layers appear to curl around their outer edges. The track is partially infilled by a thin layer of light tan limestone consistent in character with the overlying bed. The preservation grade [39, 40] of this track is 1 because the marks of the toes are distorted but visible and only the general outline of the track is clearly preserved.

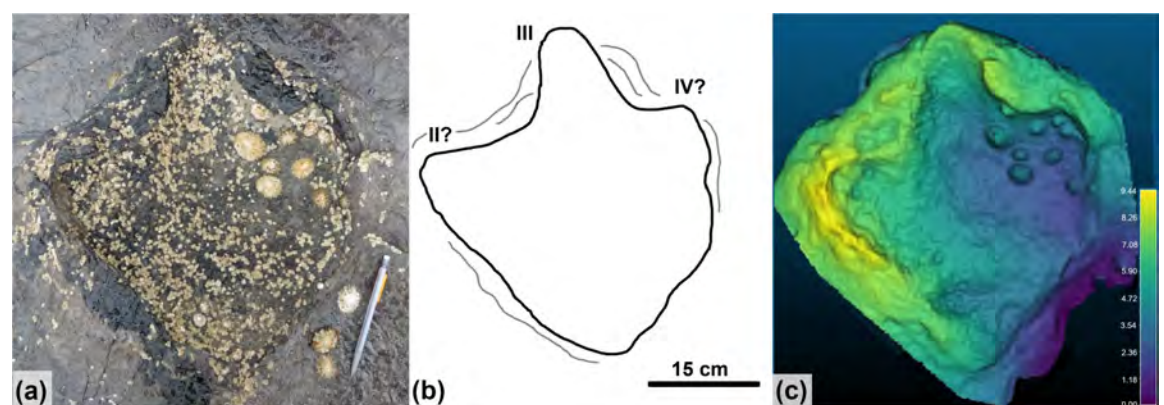


**Fig 18. Exemplar large tridactyl track (BP3\_08).** (a) A field photograph of BP3\_08 with (b) an interpretive outline and (c) a false color depth map. This track (black outline) is the most complete and diagnostic presentation of the dominant track morphotype at BP3. The light gray outlines show the areas of most intense sediment deformation. The color scale of the false color depth map is in units of cm.

<https://doi.org/10.1371/journal.pone.0229640.g018>

BP3\_08 is tridactyl, mesaxonic, and slightly asymmetric (i.e. digits II and IV are slightly different shapes). It is 40.2 cm long and 35 cm wide with an interdigital angle of  $38.5^\circ$  ( $II^{\wedge}III$ ) and  $23.8^\circ$  between digits ( $III^{\wedge}IV$ ). Thus, the angle of divarication between the lateral digits ( $II^{\wedge}IV$ ) is  $62.3^\circ$ . The assignation of digits II and IV is tentative, as this track is not part of a trackway. Since the tracks that compose BP3\_Twy\_01 exhibit a digit II that is more prominent than digit IV, a similar inference was made for numbering the digits of this isolated track. However, the existence of a slight notch below assumed digit IV might indicate that this is in fact the medial toe [95]. Since ambiguity exists in the siding of this track, the later quantitative analysis is run twice (once with the track sided as a right pes and once as the left).

BP3\_08 has a wide, broad heel and short, blunt toes with u-shaped outlines. The width of the heel is wider than the basal width of digit III. The lateral digits are nearly as wide as they are long and the length/width ratio of the track (1.15) demonstrates that these two values are nearly subequal. There is not clear curvature in the digits or evidence of a hallux impression in the smooth posterior margin of the track.

The majority of other tracks at the site broadly conform to a similar morphology to that of BP3\_08 across a varied range of completeness (some tracks are broken along the edges of the platform while others are in-filled and partially obscured by the overlying limestone bed) (Fig 19).

In addition to BP3\_08, two short tridactyl trackways (BP3\_Twy\_01 and BP3\_Twy\_02), each consisting of four tracks, are present at BP3. BP3\_Twy\_01 consists of the large tridactyl tracks BP3\_02, BP3\_03, BP3\_05, and BP3\_06. BP3\_02 and BP3\_05 (the left pes impressions of the trackway) both are truncated by the edge of the track-bearing platform and preserve remnants of the medial and one lateral digit. In both bases, the medial digit is short, blunt, and slightly longer than the lateral digit. The preserved hypices of these tracks form flattened, slightly concave scoops between the digits. Like BP3\_02 and BP3\_05, BP3\_03 preserves the medial digit and the internal lateral digit (II). However, unlike the left pes impressions of the trackway, erosion of the in-filling sediment drape is the mechanism by which the lateral digit was lost. In place of digit IV, there is a broad and shallow impression in the underlying, shale layer. BP3\_06 is unique within the BP3\_Twy\_01 as it does not have the in-filling drape of the overlying limestone that characterizes most of the tracks at this site. It consists of a shallow impression with a pronounced digit III and less distinct digits II and IV. BP3\_Twy\_01 (Fig 20 and Table 5) is oriented at  $263^\circ$  and is 3.29 meters long. The stride and pace lengths of the trackway were quite variable, with both exhibiting approximately 40 cm variability between the maximum and minimum measurements (Table 5). This variation can be explained, at least in part, by the fragmentary nature of the tracks (particularly the left pes impressions), which makes consistent measurements difficult. The average pace length of the trackway is 1.05 m and the average stride length is 2.04 m. The pace angulation of the trackway is slightly more regular and averages to  $147^\circ$ .

BP3\_Twy\_02 consists of BP3\_04, BP3\_10, BP3\_15, and BP3\_16. The primary characteristics of interest for this trackway are unusually deep heel impressions. In fact, the first track in the sequence (BP3\_04) is preserved solely as a heel impression with no clear indication of the toes. BP3\_10, BP3\_15, and BP3\_16 all are dominated by the remnants of an in-filling cast of the overlying limestone. These infilling casts hint at the remains of short, broad anteriorly directed digits, but the tracks themselves are, again, characterized by pronounced heel impressions.

Due to only the posterior margin of the BP3\_04 being preserved, this track is substantially smaller than the other tracks that compose this trackway. Strangely, although all four tracks are observed on the same bedding plane, there is no hint of an anterior margin and little of the lateral margins of BP3\_04. This difference of in the preservation between this track and subsequent ones in the trackway raises the concern that it may not, in fact, belong to the trackway.

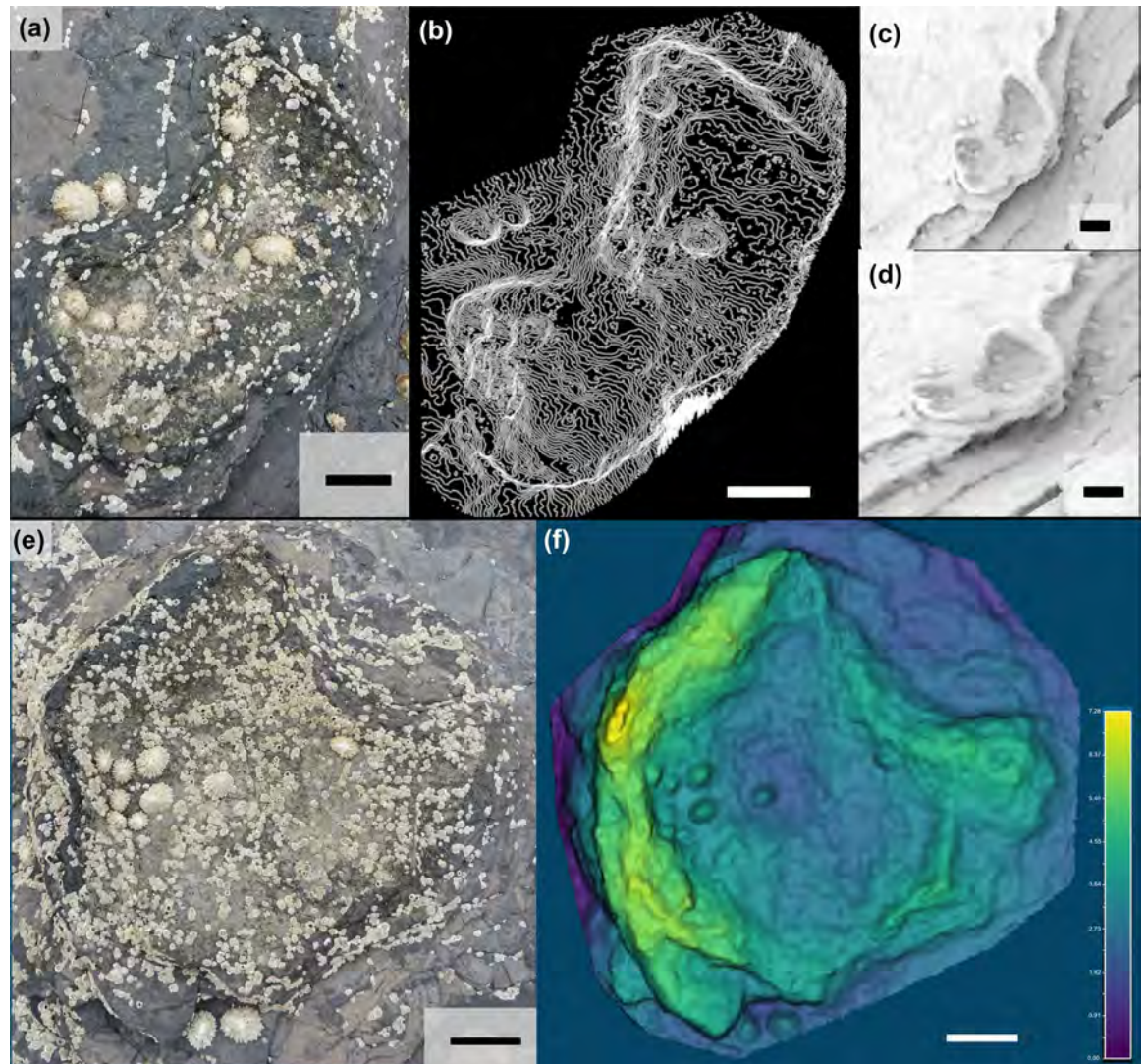


**Fig 19. Large tridactyl track preservation at BP3.** (a) A field photograph of track BP3\_05 illustrating the preservation typical of the outcrop—intense sediment deformation such that the outer margins of the track are affected by curling in the underlying shale layers. BP3\_05 is near unique within the tracksite for retaining a minimal amount of in-filling sediment with some present in the digit impressions, but otherwise little in the track. (b) Contoured (1 mm distance between lines) and (c, d) ambient occlusion renderings of the tracksite photogrammetric model highlight the presence of a ridge between the toes of BP3\_05. (e) A field photograph and (f) false color depth map of track BP3\_01 again illustrating the intense sediment deformation around the margins of the track typical at the site. All scale bars 5 cm.

<https://doi.org/10.1371/journal.pone.0229640.g019>

To combat this concern, all trackway parameters tabulated in Table 5 are calculated individually. However, notably, the stride and pace lengths measures between BP3\_04 and the subsequent 3 tracks are the most consistent of any measured from other trackways at these two sites which seems to imply that the trackway relationship between BP3\_04 and the subsequent tracks of BP3\_Twy\_02 remains a reasonable inference.

BP3\_Twy\_02 (Fig 20B) is oriented at  $350^\circ$  and is 2.70 meters long. The pace and the stride lengths of this trackway are quite regular and average to 0.734 m and 1.43 m respectively. The pace angulation of the trackway is approximately  $148^\circ$ . The preservation grade [39, 40] of the tracks that constitute BP3\_Twy\_01 ranges from 0 to 1 while the preservation grade of those that constitute BP3\_Twy\_02 is more consistently 0.

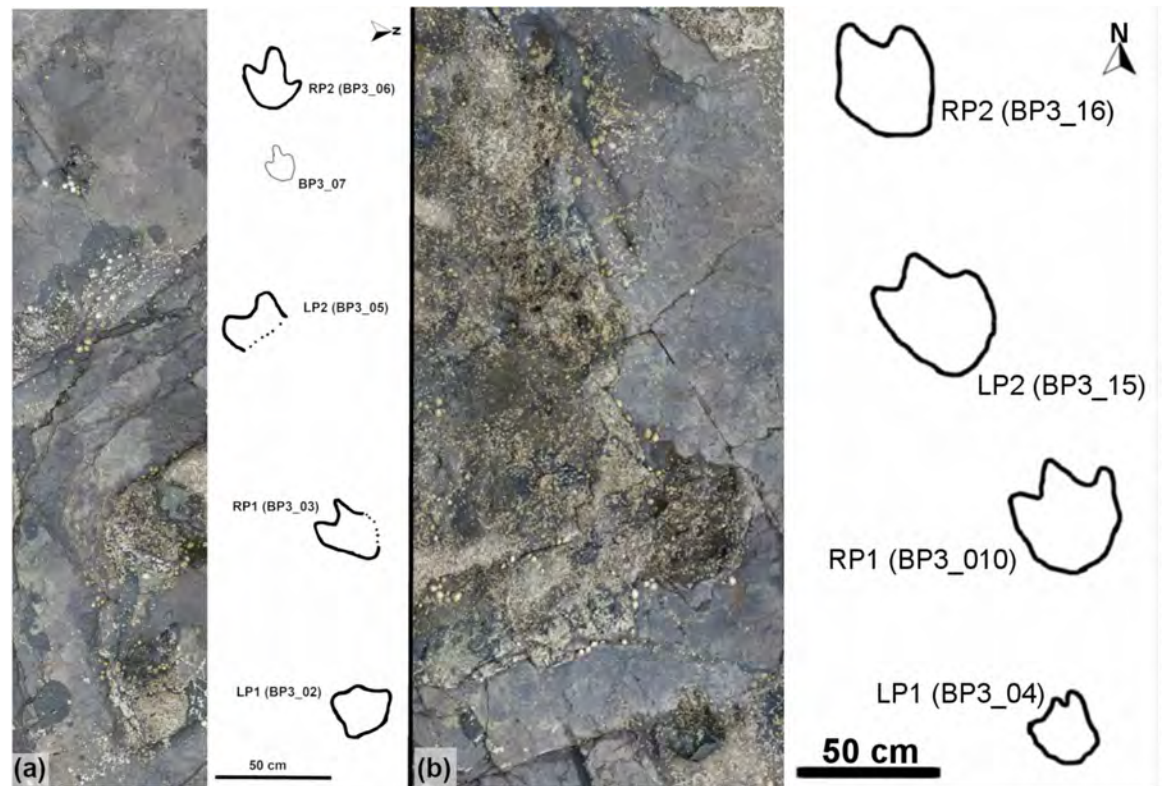


**Fig 20. Overview of trackways at BP3.** (a) BP1\_Twy\_01 shown in both the photogrammetric orthophoto and as a line drawing. The trackway consists of four, partially complete, alternating pes impressions where LP denotes the left pes and RP denotes the right pes. LP1 and RP1 are separated from LP2 and RP2 by a break in the track-bearing platform. (b) BP1\_Twy\_02 shown in both the photogrammetric orthophoto and as an outline drawing. The trackway consists of four pes impressions. LP1 is the most fragmentary track and is only preserved as a deep heel impression. This deep heel persists through the other tracks. The trackway skirts the edge of the overlying beds and, as a result, many of the features of the constituent tracks are obscured.

<https://doi.org/10.1371/journal.pone.0229640.g020>

BP3\_Twy\_01’s trackmaker hip height was calculated using the average length of the complete tracks. The average trackway stride length was 2.04 m while the relative stride length is less than 2.0. Similarly, the smaller stride length of BP1\_Twy\_02 (1.43 m) and the average of the two most complete tracks (BP3\_10 and BP3\_15) yield an even lower stride length value. These values indicate that the trackmakers were both moving at a walking pace. We

**Table 5. BP3 trackway measurements.**

	N	LP[1]	LP[2]	RP	S[1]	S[2]	WAP[1]	WAP[2]	$\gamma$ [1]	$\gamma$ [2]	$\alpha$ [1]	$\alpha$ [2]	Total Length	Orientation
BP3_Twy_01	4	0.81	1.23	1.12	1.84	2.25	0.19	0.49	150	147	60	23	3.29	260
BP3_Twy_02	4	0.72	0.72	0.77	1.41	1.45	0.12	0.16	147	150	26	10	2.70	350

The measurements made on the two trackways at BP3 are summarized here. N represents the number of tracks in the trackway. All measurements are reported in meters except for  $\gamma$ ,  $\alpha$ , and orientation which are measured in degrees. LP[1] and LP[2] represent the left pace measurements taken between LPx and RPx of the trackways respectively (track designations figured on outline drawings). RP represents the right pace measurements between RP1 and LP2. S[1] and S[2] are the stride lengths between the left feet and the right feet respectively. WAP[1] is the trackway width measured between LP1 and LP2 with RP1 as the focal point while WAP[2] is the trackway width measured between RP1 and RP2 with LP2 as the focal point.  $\gamma$  is the pace angulation with [1] using RP1 as the vertex of the angle and [2] using LP2 as the vertex of the angle.  $\alpha$  measures the track rotation of individual footprints. In this case,  $\alpha$  [1] corresponds to LP1 and  $\alpha$  [2] corresponds to RP2. The fragmentary nature of the footprints measure meant that this value could not be determined with a great deal of confidence.

<https://doi.org/10.1371/journal.pone.0229640.t005>

summarize the approximate hip heights of the trackmaking individuals and their estimated velocities in Table 6.

Due to the poor quality of preservation of BP3\_08 and the other large tridactyl tracks at the site, it is not possible to confidently assign them to a specific ichnotaxon. Since the track lengths on average are greater than 30 cm, they fall into the large, bipedal dinosaur size category. Two different trackmaker inferences are possible for the dinosaurian trackmaker of BP3\_08 –theropod or ornithopod.

A theropod trackmaker could potentially be inferred for the large tridactyl tracks at BP3 because these footprints are generally longer than they are wide which results in a narrower aspect ratio [63]. Additionally, the tracks at BP3 often present with asymmetry across the track midline with several tracks showing a disparity of  $\sim 10^\circ$  between the (II<sup>^</sup>III) and (III<sup>^</sup>IV). Asymmetry in tridactyl tracks is more strongly associated with theropod footprints (and can be employed to assist in siding isolated pes impressions) [95] while ornithopod footprints are considered more likely to be subsymmetrical [43, 66].

An ornithopod trackmaker could potentially be inferred for BP3\_08 on the basis of the track's wide, broad heel with a smooth posterior margin and its short, blunt toes with u-shaped outlines [38, 96]. The tracks lack clear curvature in the digits and evidence of claw marks or hallux impressions [96]. Additionally, the angle of divarication between the lateral digits is (II<sup>^</sup>IV) is  $62.3^\circ$  which is generally congruent with the angle of  $60^\circ$ - $65^\circ$  postulated for ornithopod trackmakers [38, 96]. In terms of trackway characteristics, the slight (inward) rotation of the pes in BP3\_Twy\_01 provides another line of evidence for a potential ornithopod trackmaker.

This trackmaker inference is further supported by the statistical parameters derived by [42], but these measurements must be regarded with caution because they are affected by the presence of infilling sediment. Sediment infilling tends result in a smoothing of the track outline and can result in tracks showing more 'ornithopod-like' features, like shorter toes and longer distances between the posterior margin of the track and the hypex. In the case of BP3\_08, the measurements of the hypices, in particular, are likely affected by the presence of infilling sediment. Table 7 summarizes the statistical parameters. For each ratio presented, BP3\_08 exhibits more ornithopod affinities.

Although the identity of the trackmaker for BP3\_08 cannot be resolved with confidence, if this track was made by an ornithopod trackmaker, some interesting implications arise that merit further discussion (see 'Implications of Potential Large Ornithopod Tracks' section below).

Although the outcrop at BP3 is dominated by large tridactyl tracks, the track assemblage at this site is not monotoxic. A second, noteworthy track morphology (small, tridactyl) is visible through a window in the overlying bioclastic limestone.

**Table 6. BP3 large bipedal trackmaker size and velocity estimations.**

	Average Approximate Trackmaker Hip Height (cm)	Estimated Velocity	
		m/s	km/hr
BP3_Twy_1	128	1.9	7.0
BP3_Twy_2	169	0.77	2.8

The range in approximate trackmaker sizes at BP3 indicates that at least two differently sized individuals were present on the mudflat. BP3\_Twy\_02's trackmaker represents the largest individual at the site and was moving at the slowest estimated velocity.

<https://doi.org/10.1371/journal.pone.0229640.t006>

Table 7. Assessment of the trackmaker affinity of BP3\_08.

IF BP3_08 IS A RIGHT PES		
Track Parameters	Threshold values and probability that the track is either theropod or ornithopod	BP3_08
L/W	80.0% Theropod > 1.25 > Ornithopod 88.2%	1.15
L/K	70.5% Theropod > 2.00 > Ornithopod 88.0%	1.10
L/M	65.0% Theropod > 2.00 > Ornithopod 90.7%	1.29
BL2/WMII	76.1% Theropod > 2.00 > Ornithopod 97.4%	1.04
BL3/WMIII	72.7% Theropod > 2.20 > Ornithopod 97.7%	1.42
BL4/WMIV	76.1% Theropod > 2.00 > Ornithopod 97.6%	1.09
LII/WBII	84.6% Theropod > 3.75 > Ornithopod 90.2%	2.88
LIII/WBIII	70.6% Theropod > 4.00 > Ornithopod 91.5%	3.79
LIV/WBIV	73.7% Theropod > 3.75 > Ornithopod 93.4%	3.35
IF BP3_08 IS A LEFT PES		
Track Parameters	Threshold values and probability that the track is either theropod or ornithopod	BP3_08
L/W	80.0% Theropod > 1.25 > Ornithopod 88.2%	1.15
L/K	70.5% Theropod > 2.00 > Ornithopod 88.0%	1.29
L/M	65.0% Theropod > 2.00 > Ornithopod 90.7%	1.10
BL2/WMII	76.1% Theropod > 2.00 > Ornithopod 97.4%	1.09
BL3/WMIII	72.7% Theropod > 2.20 > Ornithopod 97.7%	1.42
BL4/WMIV	76.1% Theropod > 2.00 > Ornithopod 97.6%	1.04
LII/WBII	84.6% Theropod > 3.75 > Ornithopod 90.2%	3.35
LIII/WBIII	70.6% Theropod > 4.00 > Ornithopod 91.5%	3.79
LIV/WBIV	73.7% Theropod > 3.75 > Ornithopod 93.4%	3.35

The calculated track parameters for BP3\_08 are summarized and compared with the likelihood analyses of [42]. Since the siding of this pes impression was equivocal, the analysis was run twice (once assuming the foot was a right pes and once with the assumption of it being a left pes). The analysis yielded the same results in both cases because the parameters of [42] propose identical thresholds for values that are symmetric across the midline (albeit with different confidences). In this case, the observed asymmetry of the track does not have a notable influence on the resultant affinity. For each parameter examined, BP3\_08 shows a stronger ornithopod affinity than a theropod affinity.

<https://doi.org/10.1371/journal.pone.0229640.t007>

**Small tridactyl track.** Track BP3\_13 (Fig 21) is a small track located west of Trackway 2, east of the small tidal pool shown on the site map with a dashed outline, and north of two large isolated boulders in the south-west corner of the platform (Fig 5). The orientation of the track's elongation axis is almost directly north. This track is not associated with the large concentration of tracks along the south edge of the platform. The track is preserved as a shallow impression in the uppermost layer of the track-bearing shale unit. The presence of a dark, biotically-derived (algal?) coating on most of the rock surface makes interpretation of this layer and the subtle features of the footprint within it difficult to interpret. The preservation grade [39, 40] of this track is 1 because the outlines of the digits are clear, but there are no clear indications of unguis marks or digital pads.

BP3\_13 is tridactyl and mesaxonic, with elongate narrow toes ending in sharp points and a narrow 'heel' with a 'v-shaped' posterior margin. No distinctive claw impressions were observed. There is no evidence of a hallux impression. The track is 8.9 cm long and 5.1 cm wide with interdigital angles of 27° between digit IV? (tentatively assigned to the right digit) and digit III and 21° between digit III and digit II? (tentatively assigned to the left digit). This track plots as having a theropod affinity according to the statistical parameters from [41] (Table 8).

The short length of this footprint places it in the tiny bipedal trackmaker size class [44] and the estimated hip height of the trackmaker is ~36 cm. BP3\_13 is the smallest track documented across both BP1 and BP3.

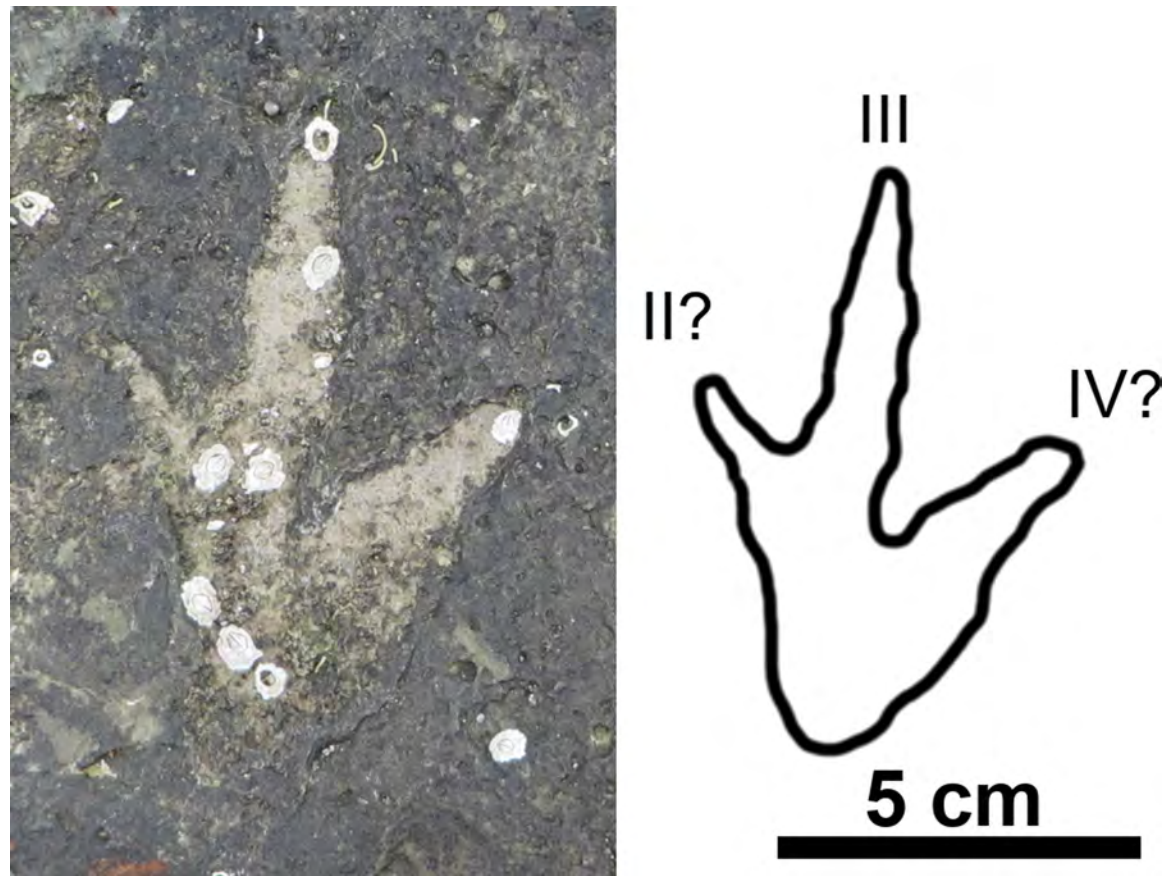


**Fig 21. Small tridactyl track from BP3 (BP3\_13).** BP3\_13 is shown with both a field photo and a line drawing. It is the smallest track at BP3. This narrow-toed track morphology—typical of Triassic and Early Jurassic tracks—is unique with regard to all other tracks at BP1 and BP3.

<https://doi.org/10.1371/journal.pone.0229640.g021>

**Table 8. Assessment of the trackmaker affinity of BP3\_13.**

Track Parameters	Threshold values and probability that the track is either theropod or ornithopod	BP3_13
L/W	80.0% Theropod > 1.25 > Ornithopod 88.2%	1.75
L/K	70.5% Theropod > 2.00 > Ornithopod 88.0%	1.93
L/M	65.0% Theropod > 2.00 > Ornithopod 90.7%	2.62
BL2/WMII	76.1% Theropod > 2.00 > Ornithopod 97.4%	2.33
BL3/WMIII	72.7% Theropod > 2.20 > Ornithopod 97.7%	4.30
BL4/WMIV	76.1% Theropod > 2.00 > Ornithopod 97.6%	3.11
LII/WBII	84.6% Theropod > 3.75 > Ornithopod 90.2%	4.55
LIII/WBIII	70.6% Theropod > 4.00 > Ornithopod 91.5%	6.85
LIV/WBIV	73.7% Theropod > 3.75 > Ornithopod 93.4%	3.12

The calculated track parameters for BP3\_13 are compared with the likelihood analyses of [42]. For the majority of the parameters examined, BP3\_13 is more likely a theropod track than an ornithopod track. The track shows a slight ornithopod affinity with regard to two parameters: LIV/WBIV and L/K. The first inconsistency occurs because the width at the base of digit IV is relatively large. This result is because of a slight outward bend along the right edge of the track. It is possible that this feature results from the eye being tricked by the growth of the dark coating on the limestone. Similarly, the L/K ratio examines the hypex distance between the digits III and II. As digit II appears to truncate into digit III quite early, the length of the hypex distance is increased. As with LIV/WBIV, it is possible that the perception of this track parameter may have been affected by the eye being drawn to areas of sharp contrast (e.g. between light and dark colors) rather than to the correct track margins.

<https://doi.org/10.1371/journal.pone.0229640.t008>

## Discussion

BP1 and BP3 preserve tracks from a variety of dinosaurian trackmakers, including bipedal theropods, possible ornithopods, and a quadrupedal ornithischian. The only major dinosaur clade that is not represented at the site is Sauropoda. The lack of sauropod tracks at these sites may be environmental as the sauropod tracks previously described from Skye [24, 25] were made in shallow lagoons and not on subaerially exposed mudflats (the depositional environments inferred for the BP1 and BP3 sites). Although sauropod tracks are not present at BP1 and BP3, the track morphologies observed at these sites (which are located in close stratigraphic and geographic proximity to one another) illustrate a diverse Middle Jurassic dinosaur fauna for Skye. These sites are currently the single best glimpse into the diversity of Skye's Middle Jurassic ecosystems because other tracksites on the island exhibit a much lower trackmaker diversity ([21] and references therein). Indeed, the desiccation surfaces on which both of these tracksites formed were likely only exposed for short periods of time before being reclaimed by the marginal lagoons. Thus, this wide diversity of dinosaurs is recorded as living more or less contemporaneously in the same environments. Although behavioral interpretations of the animals are limited by the small surface area of the outcrops and the low number of trackways present, the range of trackway orientations and lack of a preferential direction of movement on these admittedly limited exposures more strongly hints at either the time averaging of multiple generations of tracks at the site or milling behavior rather than any obvious predator-prey, migratory, or other complex behaviors. Essentially, BP1 and BP3 give us a snapshot of a 'day in the life' of a rare Middle Jurassic ecosystem.

## Implications of *Deltapodus* tracks

The *Deltapodus* sp. tracks at BP1 are the first reported examples of the ichnogenus from Skye and are among the oldest examples of this ichnotaxon from anywhere in the world. To our knowledge, the only reported *Deltapodus* tracks that are definitively older come from the Aalenian-aged type series in Yorkshire [74, 85]. All other *Deltapodus* tracks have been described from Late Jurassic to Early Cretaceous-aged sediments [56, 81–84, 86, 97, 98]. Additionally, the Skye *Deltapodus* sp. tracks are the most northerly occurrence of this ichnogenus and thus extend its geographic range (Fig 22). Therefore, the Skye tracks give important insight into the origin and early evolution of the *Deltapodus* trackmaker, widely regarded to be a thyreophoran ornithischian and most likely a stegosaur [84].

It is generally held that *Deltapodus* tracks were produced by a stegosaur, a member of the subgroup of plate-backed, beaked, plant-eating dinosaurs that includes the iconic Late Jurassic *Stegosaurus* [84]. However, there is some debate about this assignment, as other workers have proposed that the trackmaker was an ankylosaur [76, 78]. This alternative hypothesis has been based on postulated trackway characteristics (i.e. that the rotation of the pes more accurately represents ankylosaurs) and because of the shortness and bluntness of the toes which are held to be different from the more elongate toes of stegosaurs [78]. Additionally, [76] argued that presence of another aptly named ichnogenus, *Stegopodus*, with longer, more developed digits was more representative of the track morphology implied from the osteology of the stegosaurian manus and pes. They concluded that another trackmaker must, therefore, be sought for *Deltapodus* tracks.

Despite these challenges, we find the argument of stegosaurian affinity for *Deltapodus* to be most persuasive based on the number of digits in the pes. Although the ankylosaur pes has ranged from tetradactyl to tridactyl through the history of the clade, tridactyly is currently known only in the Cretaceous genera *Euoplocephalus* [100], *Pinacosaurus* [101], and *Liaoningosaurus* [102]. Most ankylosaurs, for instance, *Sauropelta* [103], have four pedal digits. Similarly, the



The strongest ichnological critique of *Deltapodus* tracks possibly not having a stegosaurian origin came from the contrast of these tracks with *Stegopodus* prints, which are widely considered to have been made by stegosaurs [76]. However, recent discoveries from China hint that some of the differences between these ichnotypes may be due to the consistency of the substrate and subsequent preservation [113]. The variable preservation of *Shemuichnus* (an early Jurassic ichnogenus attributed to ornithischians of unknown affinity) from shallow impressions that strongly resemble *Stegopodus* to deep tracks whose morphology is more consistent with *Deltapodus* has the broader implications that *Deltapodus* tracks may simply be 'deep tracks' from the same trackmaker as *Stegopodus* [84, 113]. This realization has the potential to resolve much of the apparent dichotomy between the ichnogenera. Thus, in summary, a consensus is slowly being reached between both ichnologists and osteologists regarding a likely stegosaurian affinity for *Deltapodus*.

The likely stegosaurian identity for *Deltapodus* and the identification of *Deltapodus* tracks on Skye have important implications for our understanding of Middle Jurassic dinosaur faunas and stegosaurian evolution. The *Deltapodus* sp. tracks at BP1 are the trace fossil evidence of possible stegosaurs from Skye, and the first strong indication that these dinosaurs were part of the diverse Middle Jurassic fauna of the island. A single osteological discovery—a partial ulna and radius from the Bearreraig Sandstone (a nearshore marine unit that underlies the Lealt Shale Formation)—hinted that a thyreophoran may have been present on Skye, but the fragmentary nature of these bones precluded a precise identification [9]. The bones lacked any specific diagnostic features of stegosaurs. The *Deltapodus* tracks corroborate the presence of a thyreophoran on Skye using an independent line of evidence and, specifically, point to a stegosaur.

Additional evidence of stegosaurs from the Middle Jurassic can be found with the *Deltapodus* tracks from the Aalenian in Yorkshire and body fossils including the partial skeleton of *Loricatosaurus* from the Callovian Oxford Clay Formation, vertebrae and a humerus of *Adratiklit boulahfa* from the of Bathonian of Morocco, isolated vertebrae and dermal plates from the UK referred to Stegosauria indet. and dorsal vertebrae from Kyrgyzstan referred to Stegosauria indet. [74, 112, 114–117]. Additionally, the Bajocian-aged ornithischian *Issaberrysaura mollensis* has been found as a stegosaur in recent phylogenies [118–120]. The oldest definitive ankylosaur, *Sarcolestes leedsi* is also from the Oxford Clay [121]. The presence of body fossils from Ankylosauridae (the sister group to Stegosauridae) further demonstrates that these groups had clearly diverged by the Middle Jurassic. In conjunction with these fossils, the Skye *Deltapodus* tracks suggest that stegosaurs had evolved by the Aalenian-Bajocian at latest and were already present in European and Asian ecosystems during the Middle Jurassic, before becoming larger in size and more geographically widespread later in the Jurassic.

### Implications of possible large ornithopod tracks

The large tridactyl tracks found at BP3 range in size from ~30–~40 cm, with the corresponding hip heights for the trackmakers falling between an estimated 123 and 160 cm. Notably, we did not observe any clear manus impressions in the concentration of tracks at BP3. Indeed, BP3\_Twy\_01 at this site clearly shows an alternating series of deep pes impressions only. We find no clear taphonomic reason (resulting from post-registrational processes) for manus track to be missing from this trackway if the animal was in actuality walking quadrupedally. However, the manus impressions of ornithopod tracks can often be shallow and weakly impressed into the rocks so it is possible that a bias against these features being registered in the substrate to similar depths and extents as the deep pes impressions. Based on their track size and characteristics, the animals that made these tracks might potentially have been large ornithopods that could have been at least functionally (facultatively) bipedal.

Large ornithopod footprints are not unknown from the Middle Jurassic of Skye. Indeed, the first dinosaur footprint discovered from Skye (GLAHM V1980) was derived from a layer of the Lonfearn Member of the Lealt Shale Formation very close in the stratigraphy to BP3 [22]. Although initially postulated to be a theropod track, it was later reinterpreted as being made by a large ornithopod trackmaker [22, 122]. Reexamination of GLAHM V1980 in context of this discussion proves useful because this isolated positive relief cast shows several qualitative features consistent with an ornithopod affinity. GLAHM V1980 is 45 cm long, 55 cm wide, and has wide interdigital angles (35° and 44°). It has a broad aspect ratio ( $L/W = 0.82$ ) and the presence of low, weakly developed ridges partitioning between the toes and heel. These ridges are most clearly observed in the left lateral and central digits (cf. Fig 3A of [16]). The ornithopod affinity of GLAHM v1980 seems more clearly supported than that of the *in-situ* footprints at BP3 and provides another line of evidence for the potential of large ornithopods in the Middle Jurassic of Scotland.

GLAHM V1980 was attributed to a *Camptosaurus*-like trackmaker [122] and similar-shaped footprints that reached about 70 cm in length from the Late Jurassic of Portugal were also attributed to a *Camptosaurus*-like trackmaker [64]. *Camptosaurus* is recognized as one of the most basal members of the ornithopod clade Ankylopollexia whose oldest members are known from Late Jurassic rocks [105–107].

The story told by the Skye tracks is challenging because large ornithopod footprints are predominantly found in Cretaceous-aged strata and generally are not postulated to extend much earlier in time than the Late Jurassic [43, 94]. Additionally, body fossils of the most commonly suggested trackmaker for this particular track morphology—ornithopods of similar size and phylogenetic affinity to *Camptosaurus*—are not known from the Middle Jurassic. Insight cannot be drawn from other fossils found on Skye because, in contrast to the fragmentary remains known from sauropods, theropods, and thyreophorans, no definitive ornithopod body fossils are yet known from the island.

Although scarce, Middle Jurassic-aged ornithopod body fossils are known from elsewhere in the UK, most notably a femur from the Oxford Clay of Peterborough assigned to *Callovosaurus leedsi*, which is interpreted to be a dryosaurid [123, 124]. Although dryosaurids generally had a small to medium body size (2–3 m long; [125]), it is possible that the trackmaker of GLAHM V1980 could be a large member of this clade. Although less definitive, the large tridactyl footprints at BP3 might also correspond to feet of these small-medium bodied ornithopods as the pes of these animals is narrow [126]. Alternatively, recent phylogenies of basal ornithopods recover Ankylopollexia as a sister group to Dryosauridae [105, 106, 124]. Based on these relationships, fossil evidence of dryosaurids from the Middle Jurassic implies that an ankylopollexian ghost lineage extends back into this time. Thus, the ornithopod tracks found on Skye could have been made by a smaller, primitive member of the generally large-bodied ankylopollexian clade—a ghost taxon, unrecorded by body fossils, known only from its traces.

In summary, we suggest that the trackmaker for Skye's large ornithopod tracks (if, indeed, the tridactyl footprints at BP3 and GLAHM V1980 are such) belongs to the clade Dryomorpha (the Dryosauridae + Ankylopollexian clade). It could either be a larger member of Dryosauridae or, alternatively, a small, basal ankylopollexian (*sensu* [106]). In general, 'ornithopod'-type footprints from the Early—Middle Jurassic are small (12–20 cm) [127–130] with some compelling medium to large prints known from Yorkshire [85, 131]. The ornithopod tracks found on Skye are some of the earliest potential large ornithopod footprints known from anywhere in the world, providing additional evidence for the existence of fairly large-bodied ornithopods in the Middle Jurassic and augmenting the sparse body fossil record for this time interval.

We reiterate, however, that the difficulties in distinguishing theropod and ornithopod tridactyl trackmakers means we cannot yet be fully confident that ornithopods lived on Jurassic

Skye. Future body fossil discoveries will be the best test of the ornithopod trackmaker hypothesis.

### Variations in theropod size range

Between BP1 and BP3, tridactyl tracks attributed to theropods range from the tiny size class ( $PL < 10$  cm) to the large size class ( $PL \geq 30$  cm) are described (Tables 3 and 5, S2). Conservatively, we can interpret that at least two trackmakers traversed these sites based on the size variation within the tracks. The theropods from BP1 group into medium and large bipedal dinosaur size classes with the approximate hip heights of the bipedal trackway trackmakers ranging from 116–155 cm (Table 3). In contrast, the estimated hip height for the narrow-toed trackmaker of BP3\_13 (35.6 cm) is much smaller and falls into the 'tiny' bipedal dinosaur size class. The theropod track from the site implies significantly smaller (~3 to 4 x smaller) trackmaker than the far larger tridactyl tracks located adjacently.

The substantial variation in the size of the theropod tracks at BP1 and BP3 indicates that multiple individuals left their traces on Skye's Middle Jurassic mudflats. However, identifying these trackmakers beyond the general category of 'theropod' is difficult given that there are few major osteological differences among the feet of theropods that would clearly register in tracks. Similarly varying assemblages of theropod ichnotaxa are observed in other Mesozoic tidal flats [132].

### Interpretations of dinosaur behavior

Although the presence of multiple trackways made by individuals of varying sizes shows that multiple dinosaurs traversed these mudflats, the wide variation in orientation of the trackways at both BP1 and BP3 (Fig 23) is more indicative of either different track generations (where individuals traverse the same space asynchronously and do not interact in time) or solitary behavior (milling) than any social or herd behavior (where multiple individuals travel together in a coherent manner) [133]. The trackways and isolated tracks seem randomly scattered across the outcrops and no evidence of gregariousness or interspecific interaction is observed. Speed estimations of the trackways provide slow (walking pace) velocity estimates. While the area of these outcrops, the number of trackways present, and the length of the trackways are too small to allow for confident interpretations, the trackmakers do not seem to be strongly constrained either along a coastline or by some other topographic feature.

### Insights into middle Jurassic dinosaur diversity on Skye

In the context of previously discovered dinosaur tracksites from Skye, BP1 and BP3 are remarkable for their lateral extent, the comparatively high number of tracks, and the presence of a novel ichnotaxon for the Great Estuarine Group (*Deltapodus*). The main contrast between the tracks described from BP1 and BP3 and previous discoveries lies in the novelty of the *Deltapodus* sp. tracks. Stegosaurian tracks have not been previously recognized from Skye. Additionally, the potential large ornithopod tracks provide a clearer understanding of these animals as fairly large-bodied and possibly facultatively bipedal—biological traits that are not evident from the single ornithopod footprint from Skye previously described in the literature [22, 122].

The range in size, morphology and preservation of the theropod tracks at these sites is generally consistent with previously discovered tracksites on Skye [23, 134–137]. Additionally, the subaerial mudflat where these tracks were formed generally corresponds with the depositional environments of these earlier track discoveries.

Notably, BP1 and BP3 lack any evidence of sauropod tracks. However, a recently described tracksite from slightly lower in the stratigraphy at Brothers' Point is dominated by them [25]

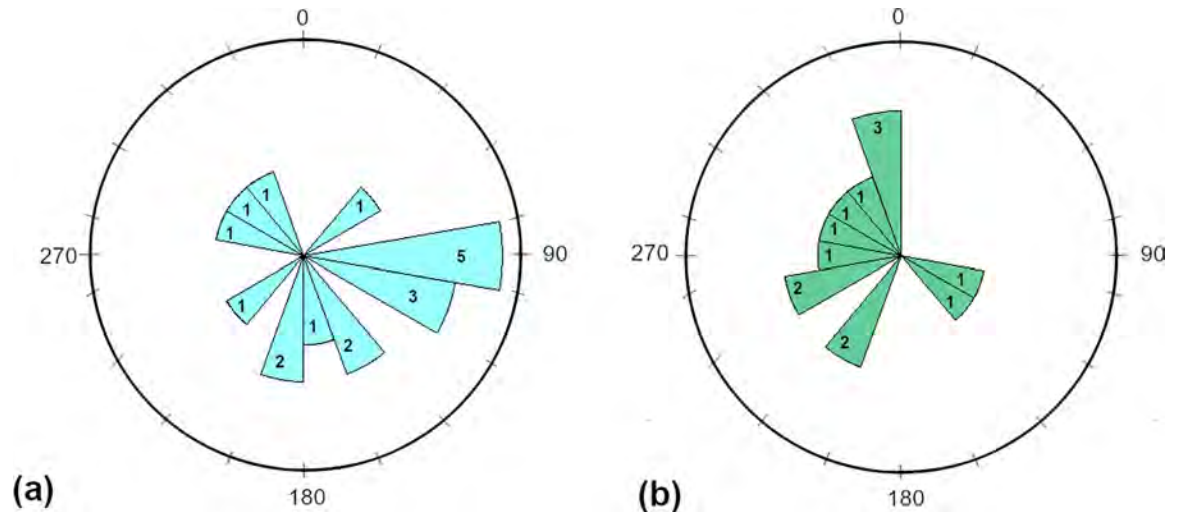


**Fig 23. Rose diagrams of track orientations for at BP1 and BP3.** Rose diagrams show the orientation of the central axis of all footprints for which this parameter could be measured from (a) BP1 and (b) BP3. These diagrams illustrate that there was no preferred direction of movement among the dinosaurs at either tracksite. The total number of tracks tabulated for BP1 was 18 and for BP3 was 13.

<https://doi.org/10.1371/journal.pone.0229640.g023>

as is another tracksite from the slightly younger Duntulm Formation [24]. When we consider the three geographically and temporally close tracksites at Brothers' Point together, we see representatives from all major dinosaur clades (theropods, sauropods, and ornithiscians).

Dinosaur tracks provide a useful complement to the body fossil record. The body fossil record on the Isle of Skye is sparse and in-situ tracksites allow better inferences to be made about the diversity, abundance, and paleobiology of dinosaurs on Skye. Tracks from Skye hint that sauropods, potentially three size classes of theropod, fairly large probable ornithopods, and possible small stegosaurs all existed relatively contemporaneously in this Middle Jurassic coastal margin environment [21] (Fig 24).

The sauropod and theropod trace fossil records of the island lend weight to the fragmentary body fossil record of these groups [8, 10–14]. Now, the *Deltapodus* sp. tracks at BP1 similarly corroborate the thyreophoran bone record [9]. However, no distinctive ornithopod skeletal material has yet been described from Skye. Thus, the Skye tracks provide evidence of a greater



**Fig 24. Reconstruction of Middle Jurassic ecosystem on the Isle of Skye, Scotland.** A snapshot of what the dynamic coastal environment of Skye may have looked like during the Middle Jurassic which bipedal ornithomimids, theropods of various sizes, and stegosaurs in the foreground and middle on subaerially-exposed mudflats. In the distance, large sauropods waded in shallow lagoons. Paleoartist: Jon Hoad.

<https://doi.org/10.1371/journal.pone.0229640.g024>

diversity of dinosaurs in this area during the Middle Jurassic than body fossils in isolation. As a result of this diversity, we can infer that a thriving community of dinosaurs lived in and near the subtropical lagoons of Middle Jurassic Scotland.

## Conclusion

We report ca. 50 dinosaur tracks from two new tracksites (BP1 and BP3) at Brothers' Point on the Isle of Skye. Both sites span two distinctive lithologies—a fine-grained shale and an overlying bioclastic limestone. At both sites, the preservation of the tracks as impressions in the shale layer with desiccation cracks propagating from the toes indicates that the track-bearing surface was subaerially exposed when the dinosaurs were walking on it. The bioclastic limestones indicate that the track-bearing surfaces were resubmerged in a lagoonal environment after desiccation. Thus, these sites show evidence of a dynamic nearshore to coastal depositional environment. Although they cover a relatively small geographic area, BP1 and BP3 show a relatively high degree of dinosaur diversity, with tracks formed by theropod, possible ornithopod, and possible stegosaurian trackmakers present.

In addition to its series of poorly preserved, large tridactyl tracks, BP3 offers a striking testament to the utility of revisiting areas that have been previously prospected, especially dynamic environments like the northern coastlines of Skye. Although this part of the coast of Port Earlish between Valtois and Brothers' Point is a popular place for tourists to walk and has been measured in detail by stratigraphers and prospected by paleontologists for almost half a century, the tracksite was not recognized until the spring storms of 2017 moved the boulders along the beach to more opportune resting places.

## Supporting information

**S1 Appendix. Additional method details, intervalometer design, model construction, and comprehensive track measurements.** This file is formatted as a .pdf and includes additional information about track measurements and description, the design of the intervalometer, a standardized workflow for constructing photogrammetric models of tracksites, and the comprehensive listing of all track measurements from BP1 and BP3. It also contains information about accessing the photogrammetric datasets associated with the project (reposited in Dryad).  
(PDF)

## Acknowledgments

We thank Matteo Belvedere, Lara Sciscio, and Brent Breithaupt for their thoughtful and constructive reviews that substantially improved the quality of this manuscript. This paper presents results from PEdP's Master's thesis at the University of Edinburgh. We thank Moji Ogunkanmi, Rachel Bartlett, Shasta Marrero, and Amelia Penny for fieldwork assistance; John Hudson and Matt Wakefield for discussions about the stratigraphic context of the sites; Tim Askew for preliminary drone images of BP1; and Sarah McGrory and Colin MacFadyen of Scottish National Heritage for arranging collection and sampling permission. We also acknowledge Minor Loan 1080 from the NERC Geophysical Research Facility for the use of GNSS survey equipment at BP1. Richard Butler and Clint Boyd provided helpful discussion on the evolution of Middle Jurassic ornithopods. Susannah Maidment and Thomas Raven gave additional insights into thyreophorans. This is PalAlba Publication Number 9.

## Author Contributions

**Conceptualization:** Stephen L. Brusatte, Thomas J. Challands.

**Investigation:** Paige E. dePolo, Stephen L. Brusatte, Thomas J. Challands, Davide Foffa, Mark Wilkinson, Neil D. L. Clark.

**Resources:** Paulo Victor Luiz Gomes da Costa Pereira, Dugald A. Ross, Thomas J. Wade.

**Visualization:** Jon Hoad.

**Writing – original draft:** Paige E. dePolo.

**Writing – review & editing:** Paige E. dePolo, Stephen L. Brusatte, Thomas J. Challands, Mark Wilkinson, Neil D. L. Clark, Thomas J. Wade.

## References

1. Weishampel DB, Barrett PM, Coria RA, Le Loeuff J, Xing X, Xijin Z, et al. Dinosaur Distribution. In Weishampel DB, Dodson P, Osmolska H, editors. *The Dinosauria*. University of California Press; 2004. <https://doi.org/10.1525/California/9780520242098.003.0027>
2. Harris JP, Hudson JD. Lithostratigraphy of the Great Estuarine Group (Middle Jurassic), Inner Hebrides. *Scott J Geol*. 1980; 16(2/3): 231–250.
3. Lloyd GT, Davis KE, Pisani D, Tarver JE, Ruta M, Sakamoto M, et al. Dinosaur and the Cretaceous terrestrial revolution. *Proc Biol Sci*. 2008; 275: 2483–2490. <https://doi.org/10.1098/rspb.2008.0715> PMID: 18647715
4. Brusatte SL, Norell MA, Carr TD, Erickson GM, Hutchinson JR, Balanoff AM, et al. Tyrannosaur paleobiology: New research on ancient exemplar organisms. *Science*. 2010; 329(5998): 1481–1485. <https://doi.org/10.1126/science.1193304> PMID: 20847260
5. Sander PM, Christian A, Clauss M, Rechner R, Gee CT, Griebeler E, et al. Biology of the sauropod dinosaurs: the evolution of gigantism. *Biol Rev*. 2011; 86: 117–155. <https://doi.org/10.1111/j.1469-185X.2010.00137.x> PMID: 21251189
6. Benson RBJ, Campione NE, Carrano MT, Mannion PD, Sullivan C, Upchurch P, et al. Rates of dinosaur body mass evolution indicate 170 million years of sustained ecological innovation on the avian stem lineage. *PLoS Biol*. 2014; 12(5): e1001853. <https://doi.org/10.1371/journal.pbio.1001853> PMID: 24802911
7. Benson RBJ. Dinosaur macroevolution and macroecology. *Ann Rev Ecol Evol Syst*. 2018; 49: 379–408. <https://doi.org/10.1146/annurev-ecolsys-110617-062231>
8. Clark NDL, Boyd JD, Dixon RJ, Ross DA. The first Middle Jurassic dinosaur from Scotland: a cetiosaurid? (Sauropoda) from the Bathonian of the Isle of Skye. *Scott J Geol*. 1995; 31(2): 171–6.
9. Clark NDL. A thyreophoran dinosaur from the Early Bajocian (Middle Jurassic) of the Isle of Skye, Scotland. *Scott J Geol*. 2001; 37(1): 19–26.
10. Liston JJ. A re-examination of a Middle Jurassic sauropod limb bone from the Bathonian of the Isle of Skye. *Scott J Geol*. 2004; 40(2): 119–122.
11. Barrett PM. A sauropod dinosaur tooth from the Middle Jurassic of Skye, Scotland. *Trans Roy Soc Edinb, Earth Sci*. 2006; 07: 25–29.
12. Wills S, Barrett PM, Walker A. New dinosaur and crocodylomorph material from the Middle Jurassic (Bathonian) Kilmaluag Formation, Skye, Scotland. *Scott J Geol*. 2014; 50(2): 183–190.
13. Brusatte SL, Clark NDL. Theropod dinosaurs from the Middle Jurassic (Bajocian-Bathonian) of Skye, Scotland. *Scott J Geol*. 2015. <https://doi.org/10.1144/sjg2014-022>
14. Clark NDL, Gavin P. New Bathonian (Middle Jurassic) sauropod remains from the Valtos Formation, Isle of Skye, Scotland. *Scott J Geol*. 2016. <https://doi.org/10.1144/sjg2015-010>
15. Waldman M, Savage RJG. The first Jurassic mammal from Scotland. *J Geol Soc, London*. 1972; 128: 119–125.
16. Evans SE, Barrett PM, Hilton J, Bulter RJ, Jones MEH, Liang M-M, et al. The Middle Jurassic vertebrate assemblage of Skye, Scotland. In: *Mesozoic Terrestrial Ecosystems: The Natural History Museum*; 2006: p.p. 36–39.
17. Anquetin J, Barrett PM, Jones MEH, Moore-Fay S, Evans SE. A new stem turtle from the Middle Jurassic of Scotland: new insights into the evolution and palaeoecology of basal turtles. *Proc. R. Soc. B*. 2009; 276: 879–886. <https://doi.org/10.1098/rspb.2008.1429> PMID: 19019789

18. Young MT, Tennant JP, Brusatte SL, Challands TJ, Fraser NC, Clark ND, et al. The first definitive Middle Jurassic atroposaurid (Crocodylomorpha, Neosuchia), and a discussion on the genus *Theriosuchus*. *Zool J Linn Soc*. 2016; 176: 443–462. <https://doi.org/10.1111/zoj.12315> PMID: 27594716
19. Panciroli E, Walsh S, Fraser NC, Brusatte SL, Corfe I. A reassessment of the postcanine dentition and systematics of the tritylodontid *Stereognathus* (Cynodontia, Tritylodontidae, mammaliamorpha), from the Middle Jurassic of the United Kingdom. *J Vertebr Paleontol*. 2017; 35(5): e1351448. <https://doi.org/10.1080/02724634.2017.1351448>
20. Yi H-Y, Tennant JP, Young MT, Challands TJ, Foffa D, Hudson JD. An unusual small-bodied crocodyliform from the Middle Jurassic of Scotland, UK, and potential evidence for an early diversification of advanced neosuchians. *Earth Environ Sci Trans R Soc Edinb*. 2017; 107(1): 1–12. <https://doi.org/10.1017/S1755691017000032>
21. Clark ND. Review of the dinosaur remains from the Middle Jurassic of Scotland, UK. *Geosciences (Basel)*. 2018; 8(53): <https://doi.org/10.3390/geosciences8020053>
22. Andrews JE, Hudson JD. First Jurassic dinosaur footprint from Scotland. *Scott J Geol*. 1984; 20(2): 129–134.
23. Clark ND, Booth P, Booth C, Ross DA. Dinosaur footprints from the Duntulm Formation (Bathonian, Jurassic) of the Isle of Skye. *Scott J Geol*. 2004; 40(1): 13–21.
24. Brusatte SL, Challands TJ, Ross DA, Wilkinson M. Sauropod dinosaur trackways in a Middle Jurassic lagoon on the Isle of Skye, Scotland. *Scott J Geol*. 2016; 52: 1–9. <https://doi.org/10.1144/sjg2015-005>
25. dePolo PE, Brusatte SL, Challands TJ, Foffa D, Ross DA, Wilkinson M, et al. A sauropod-dominated tracksite from Rubha nam Brathairean (Brothers' Point), Isle of Skye, Scotland. *Scott J Geol*. 2018; 54: 1–12. <https://doi.org/10.1144/sjg2017-016>
26. dePolo PE. In-situ tracksites on Isle of Skye (Scotland, UK) as indicators of Middle Jurassic dinosaur diversity and behavior. MScR. Thesis, The University of Edinburgh. 2017.
27. Morton N, Hudson JD. Field Guide to the Jurassic of the Isles of Rassay and Skye, Inner Hebrides, NW Scotland. In: Taylor PD, editor. *Field Geology of the British Jurassic*: Geological Society, London; 1995. Pp. 209–280.
28. Harris JP. Mid-Jurassic lagoonal delta systems in the Hebridean basins: thickness and facies distribution patterns of potential reservoir sandbodies. In: Parnell J, editor. *Basins of the Atlantic Seaboard: Petroleum Geology, Sedimentology and Basin Evolution*: Geol Soc Spec Publ. 1992; 62: 111–144.
29. Hudson JD, Wakefield MI. The Lonfearn Member, Lealt Shale Formation, (Middle Jurassic) of the Inner Hebrides, Scotland. *Scott J Geol*. 2018. <https://doi.org/10.1144/sjg2017-015>
30. Morton N, Dietl G. Age of the Garantiana Clay (Middle Jurassic) in the Hebrides Basin. *Scott J Geol*. 1989; 25(2): 153–159.
31. Riding JB. On the age of the Upper *Ostrea* Member, Staffin Bay Formation (Middle Jurassic) of north-west Skye. *Scott J Geol*. 1992; 28(2): 155–158.
32. Riding JB, Thomas JE. Marine palynomorphs from the Staffin Bay and Staffin Shale Formations (Middle-Upper Jurassic) of the Trotternish Peninsula, NW Skye. *Scott J Geol*. 1997; 33(1): 59–74.
33. Hudson JD. The recognition of salinity-controlled mollusk assemblages in the Great Estuarine Series (Middle Jurassic) of the Inner Hebrides. *Palaeontology*. 1963; 6(2): 318–326.
34. Hudson JD. The ecology and stratigraphic distribution of the invertebrate fauna of the Great Estuarine Series. *Palaeontology*. 1963; 6(2): 327–48.
35. Berner RA, De Leeuw JW, Spiro B, Murchison DG, Eglinton G. Sulphate reduction, organic matter decomposition and pyrite formation [and discussion]. *Philos Trans A Math Phys Eng Sci*. 1985; 315 (1531): 25–38.
36. Chen P-J, Hudson JD. The conchostracan fauna of the Great Estuarine Group, Middle Jurassic, Scotland. *Palaeontology*. 1991; 34(3): 515–545.
37. Leonardi G. *Glossary and Manual of Tetrapod Footprint Palaeoichnology*. Brasilia: Departamento Nacional da Producao Mineral; 1987.
38. Thulborn T. *Dinosaur Tracks*. London: Chapman and Hall; 1990.
39. Belvedere M, Farlow JO. A numerical scale for quantifying the quality of preservation of vertebrate tracks. In: Falkingham PL, Marty D, Richter A, editors. *Dinosaur Tracks: The Next Steps*. Bloomington: Indiana University Press; 2016. p. 92–98.
40. Marchetti L, Belvedere M, Voigt S, Klein H, Castanera D, Diaz-Martinez I, et al. Defining the morphological quality of fossil footprints. Problems and principles of preservation in tetrapod ichnology with examples from the Palaeozoic to the present. *Ear. Sci. Rev*. 2019; 193: 109–145. <https://doi.org/10.1016/j.earscirev.2019.04.008>

41. Schneider CA, Rasband WS, Eliceiri KW. NIH Image to ImageJ: 25 years of image analysis. *Nat Methods*. 2012; 9(7): 671–675. <https://doi.org/10.1038/nmeth.2089> PMID: 22930834
42. Moratalla JJ, Sanz JL, Jimenez S. Multivariate analysis on Lower Cretaceous dinosaur footprints: discrimination between ornithopods and theropods, *Geobios*. 1988; 21: 395–408.
43. Diaz-Martinez I, Pereda-Suberbiola X, Perez-Lorente F, Canudo JI. Ichnotaxonomic review of large ornithopod dinosaur tracks: temporal and geographic implications. *PLoS ONE*. 2015; 10(2): e0115477. <https://doi.org/10.1371/journal.pone.0115477> PMID: 25674787
44. Marty D. Sedimentology, taphonomy, and ichnology of Late Jurassic dinosaur tracks from the Jura carbonate platform (Chevenez-Combe Ronde tracksite, NW Switzerland): insights into the tidal-flat palaeoenvironment and dinosaur diversity, locomotion, and palaeoecology. PhD. Thesis, l'Universite de Fribourg. 2008.
45. Marty D, Belvedere M, Meyer CA, Mietto P, Paratte G, Lovis C, et al. Comparative analysis of Late Jurassic sauropod trackways from the Jura Mountains (NW Switzerland) and the central High Atlas Mountains (Morocco): implications for sauropod ichnotaxonomy. *Hist Biol*. 2010; 22(1–3): 109–133. <https://doi.org/10.1080/08912960903503345>
46. Salisbury SW, Romilio A, Herne MC, Tucker RT, Nair JP. The dinosaurian ichnofauna of the Lower Cretaceous (Valanginian-Barremian) Broome Sandstone of the Walmadany Area (James Price Point), Dampier Peninsula, Western Australia. *J Vertebr Paleontol*. 2016; 36 1–152. <https://doi.org/10.1080/02724634.2016.1369539>
47. Marty D, Belvedere M, Razzolini NL, Lockley MG, Paratte G, Cattin M, et al. The tracks of giant theropods (*Jurabrontes curtedulensis* ichnogen. & ichnosp. nov.) from the Late Jurassic of NW Switzerland. *Hist Biol*. 2018; 30(7): 928–956. <https://doi.org/10.1080/08912963.2017.1324438>
48. Razzolini NL, Belvedere M, Marty D, Paratte G, Lovis C, Cattin M, et al. *Megalosauripus transjuranicus* ichnosp. nov. A new Late Jurassic theropod ichnotaxon from NW Switzerland and implications for tridactyl dinosaur ichnology and ichnotaxonomy. *PLoS ONE* 2017; 12(7): e0180289. <https://doi.org/10.1371/journal.pone.0180289> PMID: 28715504
49. Lockley MG. *Tracking Dinosaurs: A New Look at an Ancient World*. Cambridge: Cambridge University Press; 1991.
50. Razzolini NL, Oms O, Castanera D, Vila B, dos Santos VF, Galobart A. Ichnological evidence of megalosaurid dinosaurs crossing Middle Jurassic Tidal Flats. *Sci Rep*. 2016; 6: 31494. <https://doi.org/10.1038/srep31494> PMID: 27538759
51. Farlow JO. Sauropod tracks and trackmakers: integrating the ichnological and skeletal records. *Zubia*. 1992; 10: 89–138.
52. Romano M, Whyte MA, Jackson SJ. Trackway Ratio: A new look at trackway gauge in the analysis of quadrupedal dinosaur trackways and its implications for ichnotaxonomy. *Ichnos*. 2007; 14(3–4): 257–270. <https://doi.org/10.1080/10420940601050014>
53. Alexander RM. Estimates of speeds of dinosaurs. *Nature*. 1976; 261: 129–130.
54. Henderson D. Footprints, trackways, and hip heights of bipedal dinosaurs—testing hip height predictions with computer models. *Ichnos*. 2003; 10(2–4): 99–114. <https://doi.org/10.1080/10420940390257914>
55. Stevens KA, Ernst S, Marty D. Uncertainty and ambiguity in the interpretation of sauropod trackways. In: Falkingham PL, Marty D, Richter A, editors. *Dinosaur Tracks: The Next Steps*. Bloomington: Indiana University Press; 2016. p. 226–243.
56. Cobos A, Royo-Torres R, Luque L, Alcalá L, Mampel L. An Iberian stegosaurs paradise: The Villar del Arzobispo Formation (Tithonian-Berriasian) in Teruel (Spain). *Palaeogeogr Palaeoclimatol Palaeoecol*. 2010; 293: 223–236. <https://doi.org/10.1016/j.palaeo.2010.05.024>
57. Alexander RM. Dinosaur biomechanics. *Proc R Soc B*. 2006; 273: 1849–1855. <https://doi.org/10.1098/rspb.2006.3532> PMID: 16822743
58. Thulborn T. The gaits of dinosaurs. In: Gillette DD, Lockley MG, editors. *Dinosaur Tracks and Traces*. Cambridge University Press; 1989 pp. 39–50.
59. Falkingham PL. Interpreting ecology and behavior from the vertebrate fossil track record. *J Zool*. 2014; 292: 222–228. <https://doi.org/10.1111/jzo.12110>
60. Razzolini NL, Vila B, Castanera D, Falkingham PL, Barco JL, Canudo JI, et al. Intra-Trackway morphological variations due to substrate consistency: The ElFrontal Dinosaur Tracksite (Lower, Cretaceous, Spain). *PLoS ONE*. 2014; 9(4):e93708. <https://doi.org/10.1371/journal.pone.0093708> PMID: 24699696
61. Castanera D, Pascual C, Razzolini R, Vila Bernat, Barco JL, Canudo JI. Discriminating between medium-sized tridactyl trackmakers: tracking ornithopod tracks in the base of the Cretaceous

- (Berriasian, Spain). PLoS ONE. 2013; 8(11): e81830. <https://doi.org/10.1371/journal.pone.0081830> PMID: 24303075
62. Lallensack JN, van Heteren AH, Wings O. Geometric morphometric analysis of intratrackway variability: a case study on theropod and ornithomimid dinosaur trackways from Munchehagen (Lower Cretaceous, Germany). PeerJ. 2016; 4:e2059. <https://doi.org/10.7717/peerj.2059> PMID: 27330855
  63. Lockley MG. New perspectives on morphological variation in tridactyl footprints: clues to widespread convergence in developmental dynamics. Geol. Quart. 2009; 54(4): 415–432.
  64. Mateus O, Milan J. Ichnological evidence for giant ornithomimid dinosaurs in the Upper Jurassic Lourinha Formation, Portugal. Oryctos. 2008; 8: 47–52.
  65. Romilio A, Salisbury SW. A reassessment of large theropod dinosaur tracks from the mid-Cretaceous (late Albian-Cenomanian) Winton Formation of Lark Quarry, central-western Queensland, Australia: A case for mistaken identity. Cret. Res. 2011; 32: 135–142. <https://doi.org/10.1016/j.cretres.2010.11.003>
  66. Lallensack JN, Engler T, Barthel HJ. Shape variability in tridactyl dinosaur footprints: the significance of size and function. Palaeontology. 2019. <https://doi.org/10.1111/pala.12445>
  67. Falkingham PL. Applying objective methods to subjective track outlines. In: Falkingham PL, Marty D, Richter A, editors. Dinosaur Tracks: The Next Steps. Bloomington: Indiana University Press; 2016. p. 72–80.
  68. Breithaupt BH, Matthews NA, Noble TA. An integrated approach to three-dimensional data collection at dinosaur tracksites in the Rocky Mountain West. Ichnos. 2004; 11(1–2): 11–26. <https://doi.org/10.1080/10420940490442296>
  69. Citton P, Romano M, Carluccio R, Caracciolo FD, Nicolosi I, Nicosia U, et al. The first dinosaur track-site from Abruzzi (Monte Cagno, Central Apennines, Italy). Cretac Res. 2017; 73: 47–50. <https://doi.org/10.1016/j.cretres.2017.01.002>
  70. Romilio A, Hacker JM, Zlot R, Poropat G, Bosse M, Salisbury SW. A multidisciplinary approach to digital mapping of dinosaurian tracksites in the Lower Cretaceous (Valanginian-Barremian) Broome Sandstone of the Dampier Peninsula, Western Australia. PeerJ. 2017; 5:e3013. <https://doi.org/10.7717/peerj.3013> PMID: 28344899
  71. Day JJ, Norman DB, Gale AS, Upchurch P, Powell HP. A Middle Jurassic dinosaur trackway site from Oxfordshire, UK. Palaeontology. 2004; 47(2): 319–348.
  72. Platt BF, Suarez CA, Boss SK, Williamson M, Cothren J, Kvamme JAC. LIDAR-based characterization and conservation of the first theropod dinosaur trackways from Arkansas, USA. PLoS ONE. 2018; 13(1):e0190527. <https://doi.org/10.1371/journal.pone.0190527> PMID: 29293618
  73. Whyte MA, Romano M. Probably sauropod footprints from the Middle Jurassic of Yorkshire, England. Gaia. 1994; 10: 15–26.
  74. Whyte MA, Romano M. Probably stegosaurian dinosaur tracks from the Saltwick Formation (Middle Jurassic) of Yorkshire, England. Proc Geol Assoc. 2001; 112: 45–54.
  75. Lockley MG, Hunt AP. Dinosaur Tracks and Other Fossil Footprints of the Western United States. New York: Columbia University Press. 1995.
  76. Gierlinski GD, Sabath K. Stegosaurian footprints from the Morrison Formation of Utah and their implications for interpreting other ornithischian tracks. Oryctos. 2008; 8: 29.46.
  77. Sternberg CM. Dinosaur tracks from Peace River, British Columbia. Nat. Mus. Can. Bull. 1932; 68: 59–85.
  78. McCrea RT, Lockley MG, Meyer CA. Global distribution of purported ankylosaur track occurrences. In: Carpenter K, editor. The Armored Dinosaurs. Indianapolis: Indiana University Press 2001.
  79. Nopsca F. Die Familien der Reptilien. Fortschritte der Geologie un Palaeontologie. 1923; 2: 1–210.
  80. Hornung JJ, Reich M. Metatetrapous valdensis Nopsca, 1923 and the presence of ankylosaur tracks (Dinosauria: Thyreophora) in the Berriasian (Early Cretaceous) of Northwestern Germany. Ichnos. 2014; 21(1): 1–18. <https://doi.org/10.1080/10420940.2013.873720>
  81. Lockley MG, Garcia-Ramos JC, Pinuela L, Avanzini M. A review of vertebrate track assemblages from the Late Jurassic of Asturias, Spain with comparative notes on coeval ichnofaunas from the western USA: implication for faunal diversity in siliciclastic facies assemblages. Oryctos. 2008; 8: 53–70.
  82. Milan J, Chiappe LM. First American record of the Jurassic ichnospecies Deltapodus brodricki and a review of the fossil record of stegosaurian footprints. J Geol. 2009; 2217: 343–348. <https://doi.org/10.1086/567363>
  83. Xing L, Lockley MG, McCrea RT, Gierlinski GD, Buckley LG, Zhang J. First record of Deltapodus tracks from the Early Cretaceous of China. Cretac Res. 2013; 42: 55–65.

84. Lockley MG, Gierlinski G, Matthews N, Xing L, Cart K. New dinosaur track occurrences from the Upper Jurassic Salt Wash Member (Morrison Formation) of southeastern Utah: Implications for thyrophan trackmaker distribution and diversity. *Palaeogeogr Palaeoclimatol Palaeoecol*. 2017; 470: 116–121. <https://doi.org/10.1016/j.palaeo.2016.12.047>
85. Whyte MA, Romano M, Elvidge DJ. Reconstruction of Middle Jurassic dinosaur-dominated communities from the vertebrate ichnofauna of the Cleveland Basin of Yorkshire, UK. *Ichnos*. 2007; 14(1–2): 117–129. <https://doi.org/10.1080/10420940601010802>
86. Belvedere M, Mietto P. First evidence of stegosaurian *Deltapodus* footprints in North Africa (Iouaridene Formation, Upper Jurassic, Morocco). *Palaeontology*. 2010; 53(1): 233–240. <https://doi.org/10.1111/j.1475-4983.2009.00928.x>
87. Castanera D, Pascual C, Canudo JI, Hernandez N, Barco JL. Ethological variations in sauropod trackways from the Berriasian of Spain. *Lethaia*. 2012. <https://doi.org/10.1111/j.1502-3931.2012.00304.x>
88. Meyer et al. 2018 *Annales Societatis Geologorum Poloniae* (2018), vol. 88: 223–241. <https://doi.org/https://doi.org/10.14241/asgp.2018.0114>
89. Wilson JA, Carrano MT. Titanosaurs and the origin of “wide-gauge” trackways: a biomechanical and systematic perspective on sauropod locomotion. *Paleobiology*. 1999; 25(2): 252–267.
90. Lockley MG, Meyer CA, dos Santos VF. *Megalosauripus* and the problematic concept of megalosaur footprints. *Gaia*. 1998; 15: 313–337.
91. Olsen PE, Smith JB, McDonald NG. Type material of the type species of the classic theropod footprint genera *Eubrontes*, *Anchisauripus*, and *Grallator* (Early Jurassic, Hartford and Deerfield basins, Connecticut and Massachusetts, U.S.A.). *J Vertebr Paleontol*. 1998; 18(3): 586–601. <https://doi.org/10.1080/02724634.1998.10011086>
92. Welles SP. Dinosaur footprints from the Kayenta Formation of northern Arizona: Plateau. 1971; 44(1) 27–38.
93. Lockley MG, Gierlinski GD, Lucas SG. *Kayentapus* revisited: Notes on the type material and the importance of this theropod footprint ichnogenus. In: Sullivan RM, editor. *Fossil Record 3*, Bull N M Mus Nat Hist Sci. 2011; 53: 330–336.
94. Lockley MG, Xing L, Lockwood JAF, Pond S. A review of large Cretaceous ornithopod tracks, with special reference to their ichnotaxonomy. *Biol J Linn Soc Lond*. 2014; 118: 721–736.
95. Farlow JO, Gatesy SM, Holtz TR, Hutchinson JR, Robinson JM. *Theropod Locomotion*. *Amer. Zool*. 2000: 40: 640–663.
96. Schulp AS, Al-Wosabi M. Telling apart ornithopod and theropod trackways: a closer look at a large, Late Jurassic tridactyl dinosaur trackway at Serwah, Republic of Yemen. *Ichnos*. 2012; 19(4): 194–198. <https://doi.org/10.1080/10420940.2012.710672>
97. Mateus O, Milan J, Romano M, Whyte MA. New finds of stegosaur tracks from the Upper Jurassic Lourinha Formation, Portugal. *Acta Palaeontol Pol*. 2011; 56(3): 651–658. <https://doi.org/10.4204/app.2009.0055>
98. Pascual C, Canudo JI, Hernandez N, Barco JL, Castanera D. First record of stegosaur dinosaur tracks in the Lower Cretaceous (Berriasian) of Europe (Oncala Group, Soria, Spain). *Geodiversitas*. 2012; 34(2): 297–312. <https://doi.org/10.5252/g2012n2a4>
99. Scotese CR. *Atlas of Earth History, Volume 1, Paleogeography*. Arlington, Texas: PALEOMAP Project; 2001.
100. Coombs WP. A juvenile ankylosaur referable to the genus *Euoplocephalus* (Reptilia, Ornithischia). *J Vertebr Paleontology*. 1986; 6(2): 162–173.
101. Currie PJ, Badamgarav D, Koppelhus EB, Sissons R, Vickaryous MK. Hands, feet, and behavior in *Pinacosaurus* (Dinosauria: Ankylosauridae). *Acta Palaeontol Pol*. 2011; 56(3): 489–504. <https://doi.org/10.4204/app.2010.0055>.
102. Xu X, Wang X-L., You H-L. A juvenile ankylosaur from China. *Naturwissenschaften*. 2001; 88: 297–300. <https://doi.org/10.1007/s001140100233> PMID: 11544897
103. Carpenter K. Skeletal reconstruction and life restoration of *Sauropelta* (Ankylosauria: Nodosauridae) from the Cretaceous of North America. *Can J Earth Sci*. 1984; 21: 1491–1498.
104. Pereda-Suberbiola X, Dantas P, Galton PM, Sanz JL. Autopodium of the holotype of *Dracopelta zbyzskii* (Dinosauria, Ankylosauria) and its type horizon and locality (Upper Jurassic: Tithonian, western Portugal). *N Jb Geol Palaont Abh*. 2005; 235(2): 175–196.
105. Butler RJ, Upchurch P, Norman DB. The phylogeny of the ornithischian dinosaurs. *J Syst Palaeontol*. 2008; 6(1): 1–40. <https://doi.org/10.1017/S1477201907002271>
106. Boyd CA. The systematic relationships and biogeographic history of ornithischian dinosaurs. *PeerJ*. 2015; 3: e1523. <https://doi.org/10.7717/peerj.1523> PMID: 26713260

107. Baron MG, Norman DB, Barrett PM. Postcranial anatomy of *Lesothosaurus diagnosticus* (Dinosauria: Ornithischia) from the Lower Jurassic of southern Africa: implications for basal ornithischian taxonomy and systematics. *Zool J Linn Soc.* 2017; 179(1): 125–168.
108. Henning E. *Kentrosaurus aethiopicus*, der *Stegosauridae* des Tendaguru. *Sitzungsberichte der Gesellschaft naturforschender Freunde*: 1915; 219–247.
109. Gilmore CW. Osteology of the armored dinosaurian in the United States National Museum, with special reference to the genus *Stegosaurus*. *United States National Museum Bulletin.* 1914; 89: 1–127.
110. Barrett PM, Maidment SCR. The evolution of ornithischian quadrupedality. *J Iber Geol.* 2017. <https://doi.org/10.1007/s41513-017-0036-0>
111. Maidment SCR, Barrett PM. Does morphological convergence imply functional similarity? A test using the evolution of quadrupedalism in ornithischian dinosaurs. *Proc R Soc B.* 2012; 279: 3765–3771. <https://doi.org/10.1098/rspb.2012.1040> PMID: 22719033
112. Galton PM. Purported earliest bones of a plated dinosaur (Ornithischia: Stegosauria): a “dermal tail spine” and a centrum from the Aalenian-Bajocian (Middle Jurassic) of England, with comments on other early thyreophorans. *N Jb Geol Palaont Abh.* 2017; 285(1): 1–10. <https://doi.org/10.1127/njgpa/2017/0667>
113. Li J, Lockley MG, Zhang Y, Hu S, Matsukawa M, Bai Z. An important ornithischian tracksite in the Early Jurassic of the Shenmu Region, Shaanxi, China. *Acta Geol Sinica.* 2012; 85(1): 1–10.
114. Galton PM, Powell HP. Stegosaurian dinosaurs from the Bathonian (Middle Jurassic) of England, the earliest record of the family *Stegosauridae*. *Geobios.* 1983; 16: 219–229.
115. Averianov AO, Bakirov AA, Martin T. First definitive stegosaur from the Middle Jurassic of Kyrgyzstan. *Palaontol Z.* 2007; 81(4): 440–446.
116. Maidment SCR, Norman DB, Barrett PM, Upchurch P. Systematic and phylogeny of Stegosauria (Dinosauria: Ornithischia). *J Syst Palaeontol.* 2008. <https://doi.org/10.1017/S1477201908002459>
117. Maidment SCR, Raven TJ, Ouarhache D, Barrett PM. North Africa’s first stegosaur: implications for Gondwanan thyreophoran dinosaur diversity. *Gondwana Res.* 2020; 77: 82–97.
118. Salgado L, Canudo JI, Garrido AC, Moreno-Azanza M, Martinez LCA, Coria RA, et al. A new primitive Neornithischian dinosaur from the Jurassic of Patagonia with gut contents. *Sci Rep.* 2017; 7: 42778. <https://doi.org/10.1038/srep42778> PMID: 28202910
119. Han F, Forster CA, Xu X, Clark JM. Postcranial anatomy of *Yinlong downsii* (Dinosauria: Ceratopsia) from the Upper Jurassic Shishugou Formation of China and the phylogeny of basal ornithischians. *J Syst Palaeontol.* 2018; 16(14): 1159–1187. <https://doi.org/10.1080/14772019.2017.1369185>
120. Raven TJ, Maidment SCR. The systematic position of the enigmatic thyreophoran dinosaur *Paranthodon africanus*, and the use of basal exemplifiers in phylogenetic analysis. *PeerJ.* 2018; 6:e4529. <https://doi.org/10.7717/peerj.4529> PMID: 29576986
121. Galton PM. *Sarcoleste leedsi* Lydekker, an ankylosaurian dinosaur from the Middle Jurassic of England. *N. Jb. Geol. Palaont. Mh.* 1983; 3: 141–155.
122. Delair JB, Sarjeant WAS. History and bibliography of the study of fossil vertebrate footprints in the British Isles: Supplement 1973–1983. *Palaeogeogr Palaeoclimatol Palaeoecol.* 1985; 49: 123–160.
123. Ruiz-Omenaca JI, Pereda-Suberbiola X, Galton PM. *Callososaurus leedsi*, the earliest dryosaurid dinosaur (Ornithischia: Euornithopoda) from the Middle Jurassic of England. In: Carpenter K, editor. *Horns and Beaks: Ceratopsian and ornithopod dinosaurs.* 2006.
124. McDonald AT. Phylogeny of basal iguanodonts (Dinosauria: Ornithischia): an update. *PLoS ONE.* 2012; 7(5): e36745. <https://doi.org/10.1371/journal.pone.0036745> PMID: 22629328
125. Norman DB. Basal Iguanodontia. In Weishampel DB, Dodson P, Osmolska H, editors. *The Dinosauria.* University of California Press; 2004. <https://doi.org/10.1525/california/9780520242098.001.0001>
126. Butler RJ, Barrett PM. Ornithopods. In: Brett-Surman MK, Holtz TR, Farlow JO, editors. *The Complete Dinosaur*, 2nd Edition. Bloomington: Indiana University Press; 2012. p. 551–566.
127. Thulborn RA. Ornithopod dinosaur tracks from the Lower Jurassic of Queensland. Alcheringa. 1994; 18(3): 247–258. <https://doi.org/10.1080/03115519408619498>
128. Lockley MG, Hunt AP, Meyer C, Rainforth EC, Schultz RJ. A survey of fossil footprint sites at Glen Canyon National Recreation Area (western USA): A case study in documentation of trace fossil resources at a national preserve. *Ichnos.* 1998; 5(3): 177–211. <https://doi.org/10.1080/10420949809386417>
129. Gierlinski GD, Menducki P, Janiszewska K, Wicik I, Boczarowski A. A preliminary report on dinosaur track assemblages from the Middle Jurassic of the Imilchil area, Morocco. *Geological Quarterly.* 2009; 53(4): 477–482.

130. Xing L, Lockley MG, Tang Y, Klein H, Zhang J, Persons WS, et al. Theropod and Ornithischian footprints from the Middle Jurassic Yanan Formation of Zizhou County, Shaanxi, China. *Ichnos*. 2015; 22(1): 1–11. <https://doi.org/10.1080/10420940.2014.985670>
131. Romano M, Clark NDL, Brusatte SL. A comparison of the dinosaur communities from the Middle Jurassic of the Cleveland (Yorkshire) and Hebrides (Skye) Basins, based on their ichnites. *Geosciences (Basel)*. 2018; 8: 327. <https://doi.org/10.3390/geosciences8090327>
132. Castanera D, Belvedere M, Marty D, Paratte G, Lapaire-Cattin M, Lovis C, et al. A walk in the maze: variation in Late Jurassic tridactyl dinosaur tracks from the Swiss Jura Mountains (NW Switzerland). *PeerJ*. 2018; 6:e4579 <https://doi.org/10.7717/peerj.4579> PMID: 29629243
133. Cohen AS, Halfpenny J, Lockley MG, Michel E. Modern vertebrate tracks from Lake Manyara, Tanzania and their Paleobiology implications. *Paleobiology*. 1993; 19(4): 433–458.
134. Clark NDL, Barco-Rodriguez JL. The first dinosaur trackway from the Valtos Sandstone Formation (Bathonian Jurassic) of the Isle of Skye, Scotland, UK. *Geogaceta*. 1998; 24: 79–82.
135. Clark NDL, Ross DA, Booth P. Dinosaur tracks from the Kilmaluag Formation (Bathonian, Middle Jurassic) of Score Bay, Isle of Skye, Scotland, UK. *Ichnos*. 2005; 12(2): 93–104. <https://doi.org/10.1080/10420940590914516>.
136. Marshall P. Theropod dinosaur and other footprints from the Valtos Sandstone Formation (Bathonian, Middle Jurassic) of the Isle of Skye. *Scott J Geol*. 2005; 41(2): 97–104.
137. Clark NDL, Brett-Surman MK. A comparison between dinosaur footprints from the Middle Jurassic of the Isle of Skye, Scotland, UK and Shell, Wyoming, USA. *Scott J Geol*. 2008; 44(2): 139–150.